A Vlasov Treatment of the 2DF Collective Beam-Beam Interaction: Analytical and Numerical Results

by

Andrey Vladimirovich Sobol

B.S., Mathematics, Novosibirsk State University, 1998
M.S., Mathematics, Novosibirsk State University, 2000
M.S., Mathematics, University of New Mexico, 2003

DISSERTATION

Submitted in Partial Fulfillment of the

Requirements for the Degree of

Doctor of Philosophy

Mathematics

The University of New Mexico

Albuquerque, New Mexico

July, 2006

Acknowledgments

This work was supported by DOE grant DE-FG02-99ER41104.

I would like to thank the members of the dissertation committee Dr. Vorobieff, Dr. Hagstrom, and Dr. Aceves for useful discussions.

I would like to thank the member of the dissertation committee Dr. Vogt for useful discussions on Chapter *2D-Vlasov Model for Collective beam-beam interaction*, helping me preparing plots, and remarks throughout the manuscript.

I would like to thank the member of the dissertation committee Dr. Dumas for helpful remarks on Chapter *The Integral Equation of the Third Kind* and proof of the averaging theorem, and for careful proofreading of the manuscript.

I would like specially to thank my adviser, the chair of the dissertation committee Dr. Ellison, who helped me so much with dissertation and during all these years while I was a graduate student at University of New Mexico.

A Vlasov Treatment of the 2DF Collective Beam-Beam Interaction: Analytical and Numerical Results

by

Andrey Vladimirovich Sobol

ABSTRACT OF DISSERTATION

Submitted in Partial Fulfillment of the
Requirements for the Degree of

Doctor of Philosophy
Mathematics

The University of New Mexico

Albuquerque, New Mexico

July, 2006

A Vlasov Treatment of the 2DF Collective Beam-Beam Interaction: Analytical and Numerical Results

by

Andrey Vladimirovich Sobol

B.S., Mathematics, Novosibirsk State University, 1998

M.S., Mathematics, Novosibirsk State University, 2000

M.S., Mathematics, University of New Mexico, 2003

Ph.D., Mathematics , University of New Mexico, 2006

Abstract

We study the evolution of counter-rotating beams of elementary particles over many turns under the collective beam-beam effect in circular accelerators both numerically and analytically. In the considered model, beams are represented by density functions in 4D phase-space, and dynamics is governed by Vlasov-type equations.

We develop a scalable parallel code in C++ using MPI that integrates these evolution equations. We use a multigrid technique to cope with the 4D quadratic interpolation, and calculate the density in slowly varying coordinates, which minimizes the amount of exchanged information and improves precision. The electromagnetic force is calculated in parallel using the conjugate gradient method.

We apply the method of averaging to the density evolution equations and rigorously prove that the solution of the averaged problem stays $O(\varepsilon)$ close to the original problem solution on $O(1/\varepsilon)$ time interval under some nonresonant condition.

Averaging leads to a nonlinear continuous-time integro-differential equation, which can be linearized and transformed to an integral equation of the third kind by Laplace transform in time and Fourier transform in action. In plasma physics, a simpler version of a third kind integral equation have been studied by Van Kampen and Case. We show that these equations can be transformed to $(I - \lambda\mathbb{K})Y = R$, where I is the identity operator, and $\mathbb{K}$ is a compact operator, and prove a Fredholm alternative theorem: *a unique solution exists for any right-hand side iff the homogeneous version of this equation has only the trivial solution.* The integral operator has a spectrum with continuous part and the corresponding generalized eigenfunctions have singularities, which makes numerical solution of these equations challenging. We develop a stable numerical scheme for discretization and numerical solution of these kind of integral equations.

Contents

List of Figures

Glossary

1D, 2D, and 4D	stand for *one, two, or four-dimensional* correspondingly when used before spaces, functions, or arrays.
1DF and 2DF	indicate the number of *degrees of freedom* of a dynamical system. 1DF system has two-dimensional phase-space, and 2DF system has four-dimensional phase-space.
IP	stands for *interaction point*.
PPD	used after numbers and stands for *points per dimension* to indicated the dimension of arrays.
MPT	stands for *Macro-Particle Tracking*, the method of simulations of beam evolution in particle colliders, in which the beams are represented by a set of macro-particles.
PF	stands for *Perron-Frobenious*, the method of simulations of beam evolution in particle colliders, in which the beams are represented by their densities.
CG	stands for *Conjugate-Gradient*.

Introduction

Accelerator physics theory and technology are involved in studying the most fundamental nature of matter: nuclear structure, quark dynamics, unified field theories, and the nature of elementary particles and the fundamental forces. Accelerator technology also has made substantial contributions to other branches of physics and technology. Electron microscopy, synchrotron light sources, and medical magnetic resonance imaging are just a few of the diverse applications of this technology.

In this dissertation, we study the density evolution of elementary particle beams in circular accelerators. We consider a model for the strong-strong beam-beam interaction of two beams, representing beams by densities in 4D phase-space, in contrast with a macro-particle approach, where beams are represented by a collection of macro-particles. We describe the physical model, present some numerical results, and prove some theorems about equations involved in the model.

In the first chapter, *2-DF Vlasov Model for Collective Beam-Beam Interaction*, we introduce the mathematical model for the 2 DF collective beam-beam interaction in the Vlasov framework. It is important in physics to find the simplest model that nevertheless contains the essential mathematical properties and computational challenges of more realistic models. The model presented here neglects many particular aspects of real accelerators: there are only two bunches, which collide only at one interaction point, and only the transversal motion of the particles within the beam

is taken into consideration, while the longitudinal motion is neglected. However the model captures essential features of the dynamics: the transversal motion occurs on a scale that is thousands of times smaller than the longitudinal motion, and in fact, for the short beam is not essential. The model considered in this dissertation can be easily extended to many bunches, and many interaction points, and it is the first and necessary step toward understanding more realistic models. This model also gives rise to some interesting mathematical problems, two of which are considered in the dissertation: the solution of the integral equation of the third kind, and an averaging approximation for the evolution of densities.

In Chapter 2, *The Integral Equation of the Third Kind*, we study existence and uniqueness of the integral equations, which play an important role in our model. These equations in their simplest form have also been considered in the famous papers on plasma physics by Van Kampen and Case. In this chapter, we show that these equations can be transformed to $(I-\lambda\mathbb{K})Y = R$, where I is the identity operator, and $\mathbb{K}$ is a compact operator, and prove an analogue to the Fredholm alternative theorem: *a unique solution exists for any right-hand side iff the homogeneous version of this equation has only the trivial solution.* As a part of the proof, a stable numerical scheme is suggested for discretization and numerical solution of this kind of integral equations, therefore answering an important practical question.

In Chapter 3, *Averaging Approach for Evolving Distributions*, we use an averaging method to study the physical model introduced in the first chapter. An averaging approach is applied to discrete-time evolution in the function space governed by an integral equation with a quasi-periodic kernel. We show that such an evolution equation can be approximated with an averaged time-independent integral equation, and rigorously prove an $O(\varepsilon)$ estimate on the time scale $O(1/\varepsilon)$. Even though these results are inspired by the physical model introduced in the first chapter, they can be trivially generalized to an arbitrary number of beams and phase-space dimensions,

and may have applications in other physical models.

In Chapter 4, we present our program that directly integrates evolution equations of this model. Execution of such code has only recently become possible because of the computational power provided by parallel computers. This code calculates the evolution of distributions in the 4-dimensional phase space with over 100 points per dimension for thousands of time-steps. Calculating density evolution in slowly varying coordinates allows an effective parallel implementation of the code. The code has been tested on the NERSC parallel computer and has shown high scalability. We discuss the algorithm, communication scheme, and some code checks in Chapter 4.

Each chapter contains an introduction with some history on the subject and the relevant references at the end. At the end of Chapters 1 and 4, we present some plots obtained from numerical computations. The major theorems are formulated in Sections 2.2, 2.3, and 3.2.

Chapter 1

2-DF Vlasov Model for Collective Beam-Beam Interaction

1.1 Derivation of the Evolution Equations

We will study the evolution of only two particle beams that interact only at one interaction point (IP). The beams are represented by densities in a 4-dimensional phase space. In our model, we ignore the change of the distributions in the longitudinal coordinates, and the distribution depends only on the spatial coordinates (x, y) of the particle in the plane perpendicular to motion and on the derivatives (x', y') of these coordinates, where primes indicate the derivatives in s, and s is the arc length measured along the closed orbit. There are two phases of the evolution of the beam.

First, at the IP, the particles of each beam receive an impulse from the electromagnetic field generated by the counter-rotating beam. The change of the position of the particles is negligibly small while the change of the momentum of the particles is significant, and we say that the particles receive a kick at the IP.

Second, the densities of the beams evolve while traveling in the ring between the interactions at the IP. We will call this part of the evolution "the evolution on the orbit". In this phase, the particles interact only with the electromagnetic field of the bending and focusing magnets. In our model, we ignore nonlinear effects, and the particles will simply rotate in the phase space. The density will change accordingly.

To describe the corresponding evolution equation, we refer to the beams as *starred* and *unstarred*. For every quantity X that describes the unstarred beam, X^* will describe the same quantity for the starred beam. The evolution equations are symmetric: the system of the equations will stay the same if we exchange starred and unstarred quantities, so we state only one equation of the equation pair; the other equation can be obtained by interchanging starred and unstarred quantities. The beams are represented by densities Ψ, Ψ^* as functions in 4-dimensional phase-space $z = (x, x', y, y')$.

To calculate the change in momentum of the particles in the starred beam, we switch to the frame of the unstarred beam. We neglect the particle motions relative to the center of the beam, and use the electrostatic formulas to calculate the electric field[1]:

$$\varphi(r) = Nq \int_{\mathbb{R}^3} \rho_3(r^\dagger) G_3(r - r^\dagger) dr^\dagger, \quad E = -\nabla\varphi, \tag{1.1}$$

where $G_3(r) = 1/|r|$ is the regular 3D Green function, ρ_3 is the density of the unstarred beam normalized to 1, N is the number of particles in the unstarred beam, and q is their charge. The subscript in ρ_3 indicates that this function depends on 3 spatial coordinates; eventually the evolution equation will be written in terms of ρ_2, which depends only on two spatial coordinates. Generally speaking, the particle changes its momentum according to $\dot{p} = q^* E$, but we assume that the time of interaction is small, and the projection of particle position on the plane perpendicular

[1]The equations are given in the Gauss System of Units.

to the particle motion is insignificant. Therefore the particle located at x at the moment $t = 0$ changes its momentum while passing through the beam according to

$$\Delta p(r) = q^* \int E(r + vt)dt, \tag{1.2}$$

(we also neglect the change of E and ρ_3 during the interaction), so

$$\Delta p(r) = q^* \int_{\mathbb{R}} Nq(-\nabla) \int_{\mathbb{R}^3} \rho_3(r^\dagger) G_3(r + vt - r^\dagger)dr^\dagger dt. \tag{1.3}$$

Assuming that we can exchange the order of integration and differentiation, we obtain

$$\Delta p(r_0) = -Nq^*q \int_{\mathbb{R}^3} \int_{\mathbb{R}} \nabla_r \rho_3(r^\dagger) G_3(r + vt - r^\dagger)dtdr^\dagger. \tag{1.4}$$

Assuming that v_1, and v_2, are negligibly small and $v_3 \approx c$, we use the property of the Green function:

$$\int_{\mathbb{R}} \nabla_r G_3(r_1, r_2, r_3 + r_3^\dagger)dr_3^\dagger = \nabla_r G_2(r_1, r_2), \tag{1.5}$$

and obtain

$$\int_{\mathbb{R}} \nabla_r G_3(r_1 + v_1 t, r_2 + v_2 t, r_3 + v_3 t,)dt = \nabla_r G_2(r_1, r_2)/v_3, \tag{1.6}$$

where $G_2(r_1, r_2) = -\ln(r_1^2 + r_2^2)$ is the 2D Green function. Then

$$\begin{aligned}
\Delta p(r_1, r_2, r_3) &= -N^*q^*q\nabla_r \int_{\mathbb{R}^3} \rho_3(r_1^\dagger, r_2^\dagger, r_3^\dagger) G_2(r_1 - r_1^\dagger, r_2 - r_2^\dagger)/v_3 dr^\dagger \\
&= -N^*q^*q\nabla_r \int_{\mathbb{R}^2} \rho_2(r_1^\dagger, r_2^\dagger) G_2(r_1 - r_1^\dagger, r_2 - r_2^\dagger)/v_3 dr^\dagger \\
&= -N^*q^*q/c\nabla_r \varphi_2,
\end{aligned}$$

where $\rho_2(r_1, r_2) = \int_{\mathbb{R}} \rho_3(r_1, r_2, r_3)dx_3$ is the 2-dimensional beam density, and φ_2 is the 2-dimensional potential. It is obvious that if $\varphi_3(r_1, r_2, r_3) = \varphi_3(r_1, r_2, -r_3)$, then

$\Delta p_{||} = 0$, but one can show that this is true for any φ_2 using the superposition principle. Since the transverse components of p are not affected by the switching of the frame, the same equation gives the change of the momentum in the starred beam as well:

$$\Delta p = -N^* q^* q / c \nabla \varphi_2, \tag{1.7}$$

and a similar equation holds for the change of the particle momentum in the unstarred beam. From now on, we will only deal with 2D densities, and therefore we will drop the subscript 2. Next we calculate the change of x':

$$\begin{aligned} x' &= \frac{dx}{ds} = \frac{dx}{dt}\frac{dt}{ds} = \frac{v_x}{v_{\text{ref}}}, \\ \frac{d}{dt}x' &= \frac{d}{dt}\frac{v_x}{v_{\text{ref}}} = \frac{d}{dt}\frac{m\gamma v_x}{\gamma m v_{\text{ref}}} = \frac{\dot{p}_x}{p_{\text{ref}}}, \end{aligned}$$

where v_{ref} and p_{ref} are the speed and momentum of the reference particle. Therefore

$$\Delta x' = \frac{\Delta p}{m\gamma c}. \tag{1.8}$$

(In the last equation, we approximated $\beta \approx 1$.) We define *beam-beam parameter* as

$$\zeta = -\frac{N^* q^* q}{\gamma m c^2},$$

and express the change of the phase-space coordinate of the particle due to the received impulse, so-called *kick*, using

$$K[\rho^*](z) = \begin{pmatrix} 0 & \frac{\partial}{\partial x}\varphi^* & 0 & \frac{\partial}{\partial y}\varphi^* \end{pmatrix}^T.$$

Here φ^* is the solution of $\Delta\varphi^* = -4\pi\rho^*$, and ρ^*, the spatial density of the kicking beam, is given by

$$\rho^*(x, y) = \int\int \Psi^*(x, x', y, y')dx'dy'. \tag{1.9}$$

The 4D-phase-space coordinate z of a particle in the unstarred beam changes at the IP and becomes $z + \zeta K[\rho^*](z)$. The kick received by a particle is produced by the electromagnetic field of the counter-rotating beam, and the argument in the square brackets indicates that $K[\rho^*](z)$ depends on the spatial density ρ^*. Two components of $K[\rho^*](z)$ are 0 because the kick does not change the spatial coordinate; the kick affects a particle independently of its momentum, therefore it only depends on the x and y coordinates.

Because the Jacobian of the transformation $z+\zeta K[\rho^*](z)$ is 1, the densities change at the IP according to

$$\Psi_{n^+}(z + \zeta K[\rho^*](z)) = \Psi_n(z), \tag{1.10}$$

Where the index n indicates revolution number (the number of turns), Ψ_n, Ψ_n^* are the densities before the kick, and Ψ_{n^+}, $\Psi_{n^+}^*$ are the densities after the kick. The kick $\zeta K[\rho^*](z)$ depends only on the spatial coordinates of the particle and changes only the momentum. Therefore it does not change the spatial density of the whole distribution. As a result, we can find the inverse operator $(I + \zeta K)^{-1}$:

$$(I + \zeta K[\rho_n^*])^{-1}(z) = (I - \zeta K[\rho_n^*])z. \tag{1.11}$$

This allows us to rewrite (1.10) in a more explicit form:

$$\Psi_{n^+} = \Psi_n \circ (I - \zeta K[\rho^*]). \tag{1.12}$$

On the second phase of the evolution, the effect of the focusing magnets leads to a change of the particle coordinates. In our model, we neglect the nonlinear effects and assume that the coordinate changes according to $z \to Rz$, where R is a 4×4 matrix with unit determinant. Therefore the density rotates in the phase space:

$$\Psi_{n+1}(Rz) = \Psi_{n^+}(z). \tag{1.13}$$

In the simplest form, R has the representation

$$R = \begin{pmatrix} \cos\nu_x & -\sin\nu_x & 0 & 0 \\ \sin\nu_x & \cos\nu_x & 0 & 0 \\ 0 & 0 & \cos\nu_y & -\sin\nu_y \\ 0 & 0 & \sin\nu_y & \cos\nu_y \end{pmatrix}. \tag{1.14}$$

Combining (1.13) and (1.12) we obtain a resulting evolution equation:

$$\Psi_{n+1} = \Psi_n \circ (I - \zeta K[\Psi_n^*]) \circ R^{-1}, \tag{1.15}$$

which is the equation for the basic physical model considered in the dissertation.

1.2 Averaging Formalism

The evolution equation (1.15) can be transformed:

$$\begin{aligned} \Psi_{n+1} \circ R^{n+1} &= \Psi_n \circ (I - \zeta K[\Psi_n^*]) \circ R^n \\ &= \Psi_n \circ R^n \circ (I - \zeta R^{-n} K[\Psi_n^*] \circ R^n), \end{aligned} \tag{1.16}$$

This suggests changing variables $\Psi_n = \Psi_n \circ R^n$, which gives

$$\Psi_{n+1} = \Psi_n \circ (I - \zeta R^{-n} \tilde{K}[\Psi_n^*] \circ R^n). \tag{1.17}$$

This is an evolution equation in the slowly varying coordinates, which is implemented in the parallel code discussed in Chapter 4. In this chapter however, our next step is to show that $R^{-n}\tilde{K}[\Psi_n^*] \circ R^n$ can be represented as an integral functional with a kernel that depends on n, which would make it suitable for the averaging procedure described in detail in Chapter 3. The following rather lengthy calculations will result in a compact formula for the turn-dependent kernel, which can be approximated with

the averaged turn-independent kernel. To simplify calculations, we will assume that R is defined by (1.14) even though this approach works with a more general class of matrices. First, we calculate

$$R^{-n}K[\Psi_n^*](z) = R^n \begin{pmatrix} 0 & \frac{\partial}{\partial x} & 0 & \frac{\partial}{\partial y} \end{pmatrix}^T \int\int\int\int G(x-x^\dagger, y-y^\dagger) \\ \Psi_n^*(x^\dagger, x'^\dagger, y^\dagger, dy'^\dagger)dx'^\dagger dy'^\dagger dx^\dagger dy^\dagger,$$

Next we express z in terms of $v = (v_{11}, v_{12}, v_{21}, v_{22})$ such that $z = R^n v$:

$$R^{-n}K[\Psi_n^*] \circ R^n(v) = \begin{pmatrix} \sin n\nu_x \frac{\partial}{\partial x} & \cos n\nu_x \frac{\partial}{\partial x} & \sin n\nu_y \frac{\partial}{\partial y} & \cos n\nu_y \frac{\partial}{\partial y} \end{pmatrix}^T \\ \int\int\int\int G(v_{11}\cos n\nu_x - v_{12}\sin n\nu_x - x^\dagger, v_{21}\cos n\nu_y - v_{22}\sin n\nu_y - y^\dagger) \\ \Psi_n^*(x^\dagger, x'^\dagger, y^\dagger, dy'^\dagger)dx'^\dagger dy'^\dagger dx^\dagger dy^\dagger = J\nabla_v H[\Psi^*](v), \tag{1.18}$$

where

$$H[\Psi_n^*, n](v) = \int\int\int\int G(v_{11}\cos n\nu_x - v_{12}\sin n\nu_x - x^\dagger, \tag{1.19} \\ v_{21}\cos n\nu_y - v_{22}\sin n\nu_y - y^\dagger)\Psi_n^*(x^\dagger, x'^\dagger, y^\dagger, dy'^\dagger)dx'^\dagger dy'^\dagger dx^\dagger dy^\dagger,$$

and

$$J = \begin{pmatrix} 0 & -1 & 0 & 0 \\ 1 & 0 & 0 & 0 \\ 0 & 0 & 0 & -1 \\ 0 & 0 & 1 & 0 \end{pmatrix}. \tag{1.20}$$

Changing the integration variable to $v^\dagger = (v_{11}^\dagger, v_{12}^\dagger, v_{21}^\dagger, v_{22}^\dagger)$ such that $z^\dagger = R^n v^\dagger$ and using $\Psi_n(v^\dagger) = \Psi_n(z)$, we obtain

$$H[\Psi, n](v) = \int G(v_{11}\cos n\nu_x - v_{12}\sin n\nu_x - v_{11}^\dagger \cos n\nu_x + v_{12}^\dagger \sin n\nu_x,$$

$$
\begin{aligned}
& v_{21}\cos n\nu_x - v_{22}\sin n\nu_x - v_{21}^{\dagger}\cos n\nu_x + v_{22}^{\dagger}\sin n\nu_x)\,\Psi(v^{\dagger})dv^{\dagger} \\
&= \int G((v_{11}-v_{11}^{\dagger})\cos n\nu_x - (v_{12}-v_{12}^{\dagger})\sin n\nu_x, ...)\,\Psi(v^{\dagger})dv^{\dagger} \\
&= \int G(A_1\cos(n\nu_x+\theta_1), A_2\cos(n\nu_y+\theta_2))\,\Psi(v^{\dagger})dv^{\dagger}, \qquad (1.21)
\end{aligned}
$$

where A_m and θ_m are short-hands for

$$
A_m = \sqrt{(v_{m1}-v_{m1}^{\dagger})^2 + (v_{m2}-v_{m2}^{\dagger})^2}, \quad \cos\theta_m = \tfrac{v_{m1}-v_{m1}^{\dagger}}{A_m}, \quad \text{where } \; m = 1, 2.
$$

Note that the kernel depends only on the difference of the arguments: $G_n(h,v) = G_n(h-v)$. It is now clear that the turn-dependent kernel

$$
G_n(h-v) = G(A_1\cos(n\nu_x+\theta_1), A_2\cos(n\nu_2+\theta_2)) \qquad (1.22)
$$

can be averaged for nonresonant ν_x and ν_y as

$$
\bar{G}(h-v) = \int_0^1\int_0^1 G(A_1\cos(2\pi t_1), A_2\cos(2\pi t_2))dt_1dt_2. \qquad (1.23)
$$

The evolution equation becomes

$$
\Psi_{n+1} = \Psi_n \circ (I - \zeta J\nabla H[\,\Psi_n^*, n]), \qquad (1.24)
$$

which can be approximated by the n-independent averaged equation

$$
\bar{\Psi}_{n+1} = \bar{\Psi}_n \circ (I - \zeta J\nabla \bar{H}[\,\bar{\Psi}_n^*]). \qquad (1.25)
$$

The validity of this approximation is discussed in detail in Chapter 3. The equations obtained from (1.25,1.24) by exchanging starred and unstarred quantities are also valid and omitted here for brevity. Derived for arbitrary G, these equations are of special interest in the physical case when

$$
G(x,y) = -\ln(x^2+y^2). \qquad (1.26)
$$

.

1.3 Vlasov-Type Continuous-Time Evolution Equation

We use Poisson brackets defined as $\{f, g\} = (\nabla f, J\nabla g)$. Equation (1.25) with its starred counterpart can be viewed as an Euler step in time for the numerical solution of the continuous-time system:

$$\begin{cases} \partial_t \tilde{\Psi} \ + \{\tilde{\Psi},\ \bar{H}[\tilde{\Psi}^*]\ \} &= 0, \\ \partial_t \tilde{\Psi}^* + \{\tilde{\Psi}^*, \bar{H}^*[\tilde{\Psi}]\} &= 0, \end{cases} \tag{1.27}$$

where $\tilde{\Psi}(\zeta n, v) \approx \bar{\Psi}_n(v)$ because its characteristic equation is

$$\dot{v} = J\nabla \bar{H}[\tilde{\Psi}^*]. \tag{1.28}$$

System (1.27) can be more easily analyzed if we switch to action-angle variables $w = (\theta_1, \theta_2, J_1, J_2)$ according to

$$v_{m1} = \sqrt{2J_m}\cos\theta_m, \quad v_{m2} = \sqrt{2J_m}\sin\theta_m, \quad \text{where } \ m = 1, 2. \tag{1.29}$$

Note that this transformation does not change the form of equations (1.24-1.28). It is obvious that any function $\Psi_e(J)$ that depends only on J is an equilibrium, however we stick with a physically adequate choice for the equilibrium distribution:

$$\Psi_e(J) = \frac{1}{4\pi^2} e^{-J_x - J_y} = \frac{1}{4\pi^2} e^{-|v|^2/2}. \tag{1.30}$$

To linearize about an equilibrium, we set $\Psi(v, t) = \Psi_e(J) + \Psi_1(v, t)$ in (1.27), assuming $\Psi_1(v, t)$ is small, and obtain

$$\begin{cases} \partial_t \Psi_1 + \{\Psi_1, \bar{H}[\Psi_e^*]\} + \{\Psi_e, \bar{H}[\Psi_1^*]\} = 0, \\ \partial_t \Psi_1^* + \{\Psi_1^*, \bar{H}^*[\Psi_e]\} + \{\Psi_e^*, \bar{H}^*[\Psi_1]\} = 0. \end{cases} \tag{1.31}$$

If we change variables to $f^+ = \Psi_1 + \Psi_1^*$, and $f^- = \Psi_1 - \Psi_1^*$, which we call the π-mode, and σ-mode respectively, we reduce (1.31) to a pair of decoupled equations:

$$\begin{cases} \partial_t f^+ + \{f^+, \bar{H}[\Psi_e]\} - \{\Psi_e, \bar{H}[f^+]\} = 0, \\ \partial_t f^- + \{f^-, \bar{H}[\Psi_e]\} + \{\Psi_e, \bar{H}[f^-]\} = 0. \end{cases} \tag{1.32}$$

To express $\bar{H}$ in the new variables, we define $D_m(J, J^\dagger, \theta^\dagger - \theta) := A_m(v^\dagger - v)$:

$$\begin{aligned} D_m^2 &= (\sqrt{2J_m^\dagger}\cos\theta_m^\dagger - \sqrt{2J_m}\cos\theta_m)^2 + (\sqrt{2J_m^\dagger}\sin\theta_m^\dagger - \sqrt{2J_m}\sin\theta_m)^2 \\ &= (\sqrt{2J_m^\dagger}\cos(\theta_m^\dagger - \theta_m) - \sqrt{2J_m})^2 + (\sqrt{2J_m^\dagger}\sin(\theta_m^\dagger - \theta_m))^2 \\ &= 2J_m^\dagger\cos^2(\theta_m^\dagger - \theta) - 4\sqrt{JJ^\dagger}\cos(\theta_m^\dagger - \theta_m) + 2J_m + 2J_m^\dagger\sin^2(\theta_m^\dagger - \theta_m) \\ &= 2J_m + 2J_m^\dagger - 4\sqrt{J_m J_m^\dagger}\cos(\theta_m^\dagger - \theta_m). \end{aligned}$$

In the second equality, we used the fact that a rotation does not change the distance between points.

Here we will use the following version of the Fourier transform

$$f_k = \frac{1}{2\pi}\int_0^{2\pi} e^{-ik\cdot\theta} f(\theta)d\theta, \quad \text{where } k \in \mathbb{Z}^2, \text{ and } f(\theta) = \sum_{k\in\mathbb{Z}^2} e^{ik\cdot\theta} f_k(\theta), \tag{1.33}$$

and Fourier representation of the kernel:

$$G(J, J^\dagger, \theta^\dagger - \theta) = \sum_{k\in\mathbb{Z}^2} e^{ik\cdot(\theta^\dagger - \theta)} G_k(J, J^\dagger), \tag{1.34}$$

where

$$\begin{aligned} G_k(J, J^\dagger) &= \frac{1}{4\pi^2}\int_{[0,2\pi]^2} \bar{G}(J, J^\dagger, \theta)e^{-ik\cdot\theta}d\theta = \frac{1}{4\pi^2}\times \\ &\int_{[0,2\pi]^2}\int_{[0,1]^2}\int\int G(D_1(J, J^\dagger, \theta)\cos 2\pi t_1, D_2(J, J^\dagger, \theta)\cos 2\pi t_2)e^{-ik\cdot\theta}dt_1 dt_2 d\theta_1 d\theta_2. \end{aligned} \tag{1.35}$$

Now one can see that $\bar{H}[f]$ works on Fourier modes of f independently:

$$\begin{aligned}\bar{H}[\Psi](v) &= \int\int \bar{G}(J, J^\dagger, \theta^\dagger - \theta)\Psi(J^\dagger, \theta^\dagger)dv^\dagger \\ &= \int\int \sum_k e^{ik\cdot(\theta^\dagger-\theta)} G_k(J, J^\dagger) \sum_n e^{in\cdot\theta^\dagger} f_n(J^\dagger)dJ^\dagger d\theta^\dagger \\ &= (2\pi)^2 \int \sum_k e^{-ik\cdot\theta} G_k(J, J^\dagger) f_{-k}(J^\dagger)dJ^\dagger \\ &= (2\pi)^2 \int \sum_k e^{ik\cdot\theta} G_{-k}(J, J^\dagger) f_k(J^\dagger)dJ^\dagger,\end{aligned}$$

which allows us to solve (1.32) mode by mode:

$$\partial_t f_k + i\Omega(J)\cdot\nabla_\theta f_k - \eta(2\pi)^2 i(k\cdot\nabla\Psi_e)\int_{\mathbb{R}^2_+} G_{-k}(J, J^\dagger) f_k(t, J^\dagger)\, dJ^\dagger = 0, \quad (1.36)$$

where $\Omega(J) := \nabla_J \bar{H}[\Psi_e](J)$, and f_k stands for either f_k^+ or f_k^-, and $\eta = 1$ or $\eta = -1$ correspondingly. We use the Laplace transform

$$\hat{f}(s) = \int_0^\infty e^{-ts} f(t)dt, \quad (1.37)$$

which has the property $\widehat{f^\dagger}(s) = \hat{f}(s)s - f(0)$, to remove time dependence in (1.36):

$$s\hat{f}_k(s, J) + i\hat{f}_k(s, J)k\cdot\Omega(J) - 4\pi^2\eta(\nabla_J\Psi_e\cdot ik)\int G_{-k}(J, J^\dagger)\hat{f}_k(s, J^\dagger)dJ^\dagger = f_k(0, J),$$

where the right-hand side comes from initial conditions for (1.32). Multiplying (1.36) by i gives

$$is\hat{f}_k(s, J) - \hat{f}_k(s, J)k\cdot\Omega(J) + 4\pi^2\eta(\nabla_J\Psi_e\cdot k)\int G_{-k}(J, J^\dagger)\hat{f}_k(s, J^\dagger)dJ^\dagger = if_k(0, J).$$

Changing variables $s = -iw$ ($is = w$) gives

$$(w - k\cdot\Omega(J))\hat{f}_k(J) + 4\pi^2\eta(\nabla_J\Psi_e\cdot k)\int G_{-k}(J, J^\dagger)\hat{f}_k(-iw, J^\dagger)dJ^\dagger = if_k(0, J). \quad (1.38)$$

Assuming that $\xi := \text{sign}(\nabla_J \Psi_e(J) \cdot k)$ does not depend on J, we can rewrite the last equation in terms of

$$\begin{aligned} g(w, J) &:= \frac{\hat{f}_k(-iw, J)}{\sqrt{|\nabla_J \Psi_e(J)|}}, \\ K_k(J, J^\dagger) &:= (2\pi)^2 G_{-k}(J, J^\dagger) \sqrt{|\nabla_J \Psi_e(J) \cdot k| \quad |\nabla_J \Psi_e(J^\dagger) \cdot k|}, \end{aligned} \tag{1.39}$$

and therefore obtain a version of (1.38) with symmetric kernel:

$$(w - \Omega(J)) g(w, J) + \eta\xi \int K_k(J, J^\dagger) g(w, J^\dagger) dJ^\dagger = \frac{i f(0, J)}{2\pi \sqrt{|\nabla_J \Psi_e(J)|}}. \tag{1.40}$$

If ω is outside of the range of $k \cdot \Omega(J)$, (1.40) can be reduced to an integral equation of the second kind by a simple algebraic transformation. Conversely, if ω is in the range of $k \cdot \Omega(J)$, then (1.40) is a third kind integral equation considered in detail in Chapter 2.

1.4 Numerical Calculation of the Spectrum

The numerical computation of functions $\Omega(J)$ and $K_k(J, J^\dagger)$ is expensive: the computation of $\Omega(J)$ involves a 6-fold integral at each point of the 2D mesh, and the computation of K_k involves a 4-fold integral at each point of a 4D mesh; in this section, we discuss computation of $\Omega(J)$ and $K_k(J, J^\dagger)$, and consider a straightforward discretization of this particular equation and underline the involved difficulties. In Chapter 2, we address the existence and uniqueness of the solution of the third kind integral equation in a much more general case. In Chapter 2, we also give a stable numerical scheme for discretization of such equations, and prove that a finite dimensional approximation converges to the original problem.

The straightforward approach to discretizing (1.40) and solving the associated finite dimensional matrix eigenproblem seems to lead to reasonable results. In the

one-dimensional case, such calculations have been done in [1, 2, 3], and excellent agreement has been obtained between the FFT spectrum of a full-blown simulation and the eigenvalues of a discretization of a 1 degree-of-freedom version of (1.40). A similar approach can be used in the 2 DF case.

We found a way to simplify the calculation for general K_k, and reduce the 4-fold integral to a 2-fold integral (see Appendix C). The same kernel is involved in computing Ω, and we obtain the same improvement in the numerical calculation of Ω. However, going to meshes larger than 60 points per dimension seems computationally prohibitive. For the important particular choice of Ψ_e given by (1.30), which corresponds to an axially symmetric Gaussian distribution, we found a very simple formula involving modified Bessel functions:

$$\bar{H}[\Psi_e](J) = \int_0^\infty \frac{1}{2+q}\left(1 - \exp\left(-\frac{J_x+J_y}{2+q}\right) I_0\left(\frac{J_x}{2+q}\right) I_0\left(\frac{J_y}{2+q}\right)\right) dq.$$

The proof of this formula is given in Appendix B. This formula has been known in the context of the weak-strong tune shift.

We transform actions $I_x = J_x/(1+J_x)$ and $I_y = J_y/(1+J_y)$, thereby mapping $\mathbb{R}_+ \to [0,1)$, and use a 60×60 mesh to better capture the shape of $\Omega(J)$. The discretization of $\Omega_1(J) = \frac{\partial}{\partial J_1}\bar{H}[\Psi_e](J)$ is shown in Figure 1.4. A straightforward proof yields that

$$\lim_{|J|\to 0} \Omega_1(J) = -1/2, \quad \lim_{|J|\to\infty} \Omega_1(J) = 0, \tag{1.41}$$

and the range of $\Omega_1(J)$ is $(0;1)$ (see Appendix B).

The finite dimensional approximation of the spectrum of (1.40) is shown in Figure 1.2. The plot suggests that (1.40) has a continuous spectrum, which coincides with the range of $\Omega_1(J)$. In addition, the σ-mode has a discrete eigenvalue $\omega = 0$, and the π-mode has a discrete eigenvalue $\omega \approx 1.21$. Figures 1.4 and 1.3 show that these

eigenvalues correspond to the regular eigenfunctions. The code that tracks the phase space densities directly in 4D phase space described in Chapter 4 shows that there is a peak in the tune diagrams for π and σ-modes corresponding to these two eigenvalues. This indicates excellent agreement between these completely different approaches.

However, the algorithm does not converge as the mesh is refined beyond some limit because the original operator in (1.40) has a continuous spectrum, as suggested by Figure 1.2. The numerically computed "eigenfunctions" associated with the continuous spectrum (Figure 1.5) in fact show singular behavior at finite J, which is expected [5, 6]. A stable numerical scheme that handles these difficulties is described in Chapter 2.

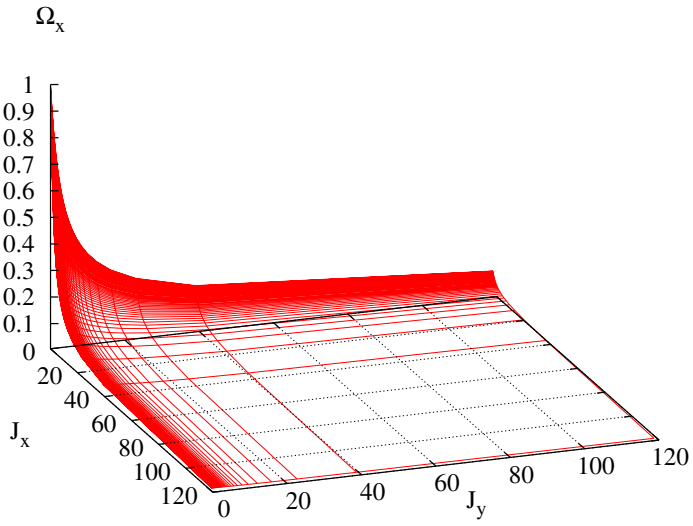

Figure 1.1: $-2\Omega_1(J)$ Plot

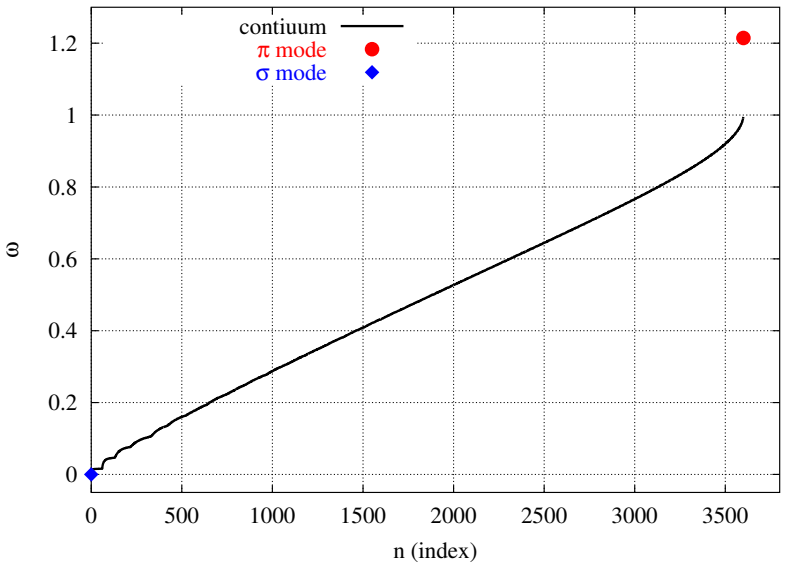

Figure 1.2: The Dipole Spectrum

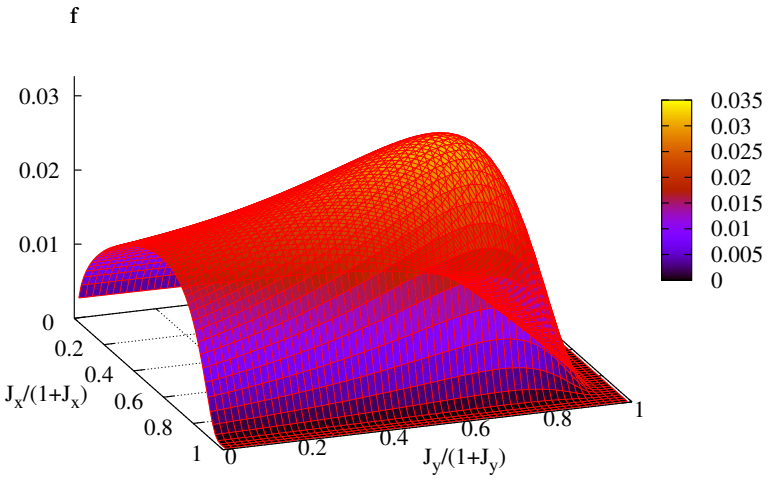

Figure 1.3: The π-mode eigenfunction

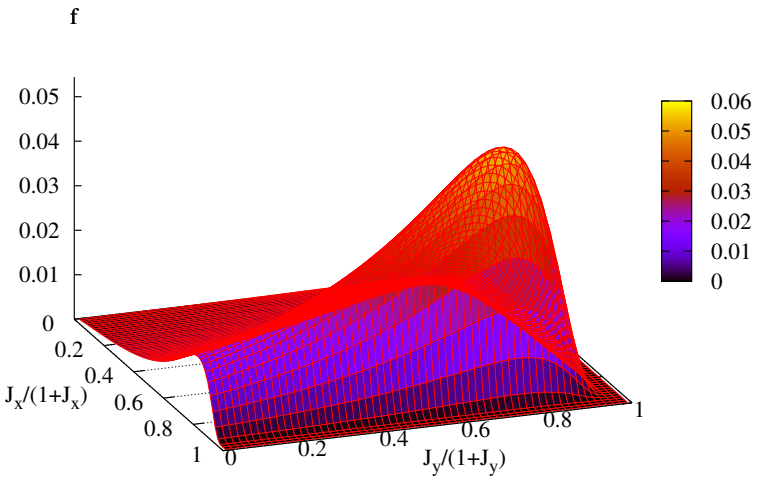

Figure 1.4: The σ-mode eigenfunction

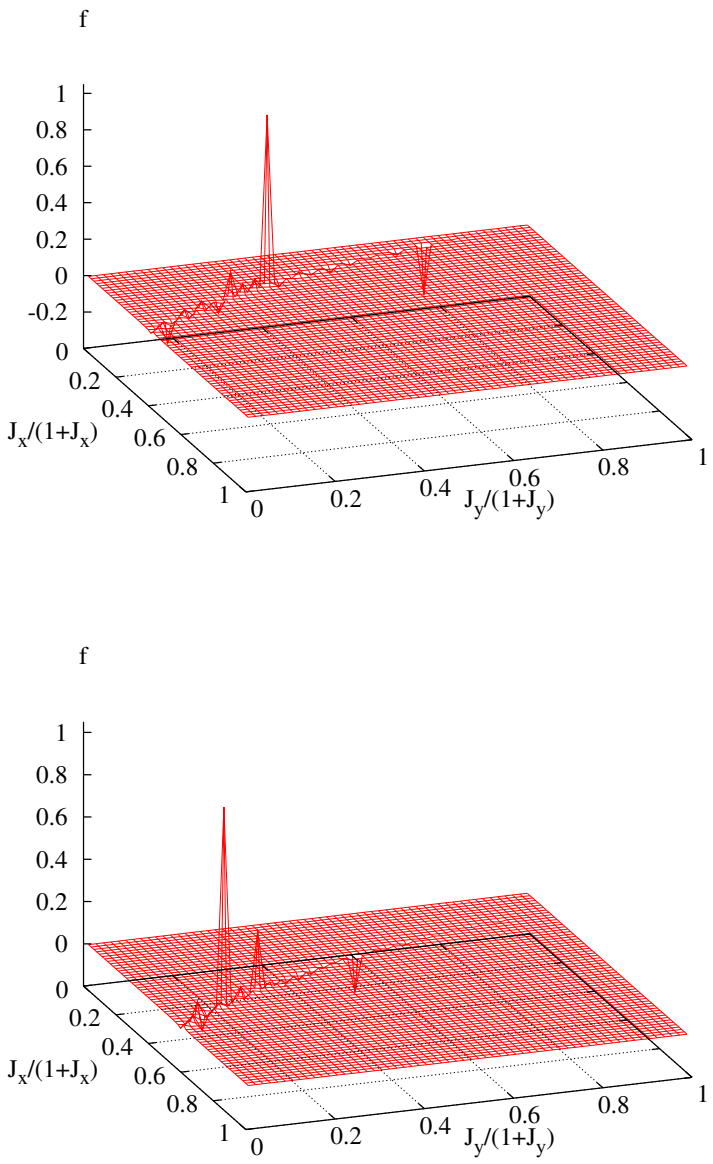

Figure 1.5: An eigenfunction corresponding to a value from the "continuous" spectrum.

References

[1] K. Yokoya and H. Koiso. *Part.Acc.*, (27):181–186, 1990.

[2] Y. Alexahin. In *LHC99 Beam–Beam workshop*, pages 41–44. CERN, 1999.

[3] M. Vogt, J. A. Ellison, T. Sen and R. L. Warnock *Two Methods for Simulating the Strong-Strong Beam-Beam Interaction in Hadron Colliders* In *Beam-Beam workshop at Fermilab*. FNAL, 2001.

Chapter 2

The Fredholm Alternative Theorem and a Stable Numerical Scheme for the Solution of Integral Equations of the 3rd Kind

2.1 Introduction

In this chapter, we solve integral equations of the form

$$g(t)\varphi(t) - \lambda \int_a^b K(t,t')\varphi(t')dt' = f(t), \tag{2.1}$$

where $a, b \in \mathbb{R}$, $g, f : [a,b] \to \mathbb{R}$, and $K : [a,b]^2 \to \mathbb{R}$ are smooth functions. In the case where g(t) has no zero, it is possible to reduce (2.1) to a Fredholm equation of the 2nd kind by simple algebraic transformations. The case where $g(t)$ has zeros is more complicated. The interest in these equations arises because of their applications in physics (see [1], [2], [3], [4]), and the necessity to solve them numerically. The goal is

to prove an analogue of the Fredholm alternative theorem and develop a convergent scheme for the numerical solution of (2.1).

These equations have been studied much less than Fredholm equations of the 2nd kind. A review of previous work on this equation was given in [5], where it was named "the integral equation of the 3rd kind".

One of the difficulties is that the space of continuous functions is not suitable for this problem and we have to choose the appropriate space of functions φ. It turns out that the appropriate space for this equation must contain either delta functions or $\frac{1}{x}$-type singularities, which presents difficulties in the numerical solution of this equation.

In [5] and [6], the possibility of solving this equation was considered in two different spaces and an analogue of the Fredholm alternative theorem was proved, however with some restrictions. Here we solve this problem in one of the spaces suggested in [5] and [6] in Section 2. We will have fewer restrictions on g, K, and f, and we extend our approach to the multidimensional case in Sections 3 and 4.

Let $\tau := \{t_i | i = 1, ..., n\}$ be the set of roots of $g(t) = 0$. We will look for solutions in the space $\mathcal{P}_\tau$, which consists of functions that have singularities at points $t_i \in \tau$. Such functions $\varphi \in \mathcal{P}_\tau$ have the convenient representation

$$\varphi(t) = \sum_i \frac{\rho_i p_i(t)}{g(t)} + y(t) \tag{2.2}$$

for some numbers ρ_i and some continuous function $y(t)$. The functions $p_i(t)$ are arbitrary except that they are required to be continuous in $[a, b]$, continuously differentiable at each t_j, and to satisfy

$$p_i(t_j) = \delta_{ij}. \tag{2.3}$$

In this chapter, the integral over singularities must be understood in the principle value sense, and we will omit the limit of the integrals and sums when it is obvious what they are. We will use $\mathcal{C}(S)$ to denote the set of continuous functions on S, and $\mathcal{C}_1(S)$ to denote the set of continuously differentiable functions. For example, the statement $g \in \mathcal{C}[a,b] \cap \mathcal{C}_1(N_\varepsilon)$ means that the function g is continuous on $[a,b]$ and continuously differentiable in the set N_ε.

This chapter is organized as follows. In the next section, we consider the case where $f(t)$ is defined on $[a,b]$, allowing $g(t) = 0$ to have any finite number of roots, and prove the Fredholm alternative theorem without restrictions, as in [6]. Unlike the approach used in [5], our approach allows us to consider the case where $t \in (a_1,b_1) \times (a_2,b_2) \subset \mathbb{R}^2$, which is done in Section 3. In Section 4, we discuss some further generalizations. We discuss numerical schemes for approximate solutions of these integral equations at the end of Sections 2 and 3. We give the proofs of Lemmas 1-5 in the last section because they contain somewhat tedious computations and the reader will probably not be interested in the details of their proof at the first reading. These lemmas are used in the proofs of the theorems in Sections 2 and 3 to insure that the smoothness conditions of the theorems are sufficient.

2.2 The 1-Dimensional Case

In the following theorem, we state very explicitly smoothness assumptions on the functions. Even though the conditions are lengthy, they are natural and easy to check. These assumption are the weakest possible in the sense that they can be replaced with a fewer number of stronger assumptions.

In this section, a continuous function $g(t)$ is defined on the interval $[a,b]$, and K is defined in $[a,b]^2$. To formulate the theorem, we introduce τ to denote the set of

all roots of $g(t) = 0$ on $[a, b]$:

$$\tau = \{t | g(t) = 0\}, \tag{2.4}$$

and N_ε to denote a union of ε-neighborhoods around points $t_j \in \tau$:

$$N_\varepsilon := \{t | \exists j \text{ s.t. } |t - t_j| < \varepsilon\} \text{ for } \varepsilon > 0. \tag{2.5}$$

Theorem Assume that for some $\varepsilon > 0$, the following conditions hold:

(r1) $g \in \mathcal{C}[a, b] \cap \mathcal{C}_2(N_\varepsilon)$,

(r2) τ is the finite set of all roots of $g(t) = 0$ on [a,b], and $a, b \notin \tau$,

(r3) $\inf_{N_\varepsilon} |g'(y)| = M_1 > 0$,

(r4) $\sup_{N_\varepsilon} |g''(y)| = M_3 < \infty$,

(r5) $p_i \in \mathcal{C}_1(N_\varepsilon) \cap C[a, b]$,

(r6) $K \in \mathcal{C}([a, b]^2)$,

(r7) $\frac{\partial}{\partial t'} K(t, t')$ exists in $[a, b] \times N_\varepsilon$, and $\sup_{[a,b]\times N_\varepsilon} |\frac{\partial}{\partial t'} K(t, t')| = M_2 < \infty$,

(r8) $\frac{\partial^2}{\partial t \partial t'} K(t, t')$ exists in $[a, b] \times N_\varepsilon$, is continuous at least at one point inside $[a, b] \times N_\varepsilon$, and $\sup_{[a,b]\times N_\varepsilon} |, \frac{\partial^2}{\partial t \partial t'} K(t, t')| = M_4 < \infty$,

(r9) $\frac{\partial}{\partial t} K(t, t')$ exists in $N_\varepsilon \times [a, b]$, and $\sup_{N_\varepsilon \times [a,b]} |\frac{\partial}{\partial t} K(t, t')| = M_5 < \infty$.

(r10) $f \in \mathcal{C}[a, b] \cap \mathcal{C}_1(N_\varepsilon)$.

Then

(a) equation (2.1) can be viewed as $(I - \lambda\mathbb{K})Y = R$, with I being the identity operator, and $\mathbb{K}$ being a compact operator, and

(b) equation (2.1) has a solution for each $y \in \mathcal{P}_\tau$ iff the homogeneous version of equation (2.1) has only the trivial solution.

Proof

We substitute (2.2) in (2.1):

$$\sum_i \rho_i p_i(t) + g(t)y(t) - \sum_i \lambda \int \frac{K(t,t')p_i(t')dt'}{g(t')}\rho_i - \lambda \int K(t,t')y(t')dt' = f(t), \quad (2.6)$$

Define

$$v_i(t) := P.V. \int \frac{K(t,t')p_i(t')dt'}{g(t')}. \quad (2.7)$$

Evaluating (2.6) at $t = t_j$, we obtain

$$\rho_j - \lambda \sum_{ij} v_i(t_j)\rho_i - \lambda \int K(t_j,t')y(t')dt' = f(t_j). \quad (2.8)$$

We multiply (2.8) by $p_j(t)$ and sum over j:

$$\sum_j \rho_j p_j(t) - \lambda \sum_{ij} p_j(t)v_i(t_j) - \lambda \sum p_j(t) \int K(t_j,t')y(t')dt' = \sum f(t_j)p_j(t). \quad (2.9)$$

Subtracting (2.9) from (2.6) and dividing by $g(t)$, we obtain

$$\begin{aligned} &y(t) - \lambda \sum_i \frac{v_i(t) - \sum_j p_j(t)v_i(t_j)}{g(t)}\rho_i \\ &\quad -\lambda \int \frac{K(t,t') - \sum_j K(t_j,t')p_j(t)}{g(t)}y(t')dt' = \frac{f(t) - \sum_j f(t_j)p_j(t)}{g(t)}. \end{aligned} \quad (2.10)$$

For convenience, define

$$u_i(t) := \frac{v_i(t) - \sum_j p_j(t) v_i(t_j)}{g(t)}, \tag{2.11}$$

$$H(t,t') := \frac{K(t,t') - \sum_j K(t_j,t') p_j(t)}{g(t)}, \tag{2.12}$$

$$F(t) := \frac{f(t) - \sum_j f(t_j) p_j(t)}{g(t)}. \tag{2.13}$$

Using these definitions, we can rewrite (2.10) as

$$y(t) - \lambda \sum_i u_i(t)\rho_i - \lambda \int H(t,t')y(t')dt' = F(t). \tag{2.14}$$

We now show that the singularities in the equation (2.10) are removable, and the functions $H(t,t')$, and F can be extended continuously. Lemma 5 in section 5 guarantees that $v \in \mathcal{C}_1(N_\varepsilon)$. The functions u_i, and F are continuous because of condition (2.3) on the choice of $p_i(t)$. Also, for any $\varepsilon > 0$, $H(t,t')$ is continuous in $[a,b]\backslash N_\varepsilon) \times [a,b]$. Because of condition (r10), the $\lim_{t\to t_j} H(t,t')$ exists. Therefore $H(t,t') \in \mathcal{C}([a,b]^2)$.

The integral operator in (2.14) is compact because H satisfies

(i) $\sup_t \int |H(t+\delta,t') - H(t,t')|dt' \to 0, \quad \text{as} \quad \delta \to 0,$

(ii) $\sup_t \int |H(t,t')|dt' < \infty.$

Note that the same conditions hold for K, which guarantees that the integral operators in (2.8) and (2.14) are compact in $\mathcal{C}$. Now we rewrite (2.8) and (2.14) side by side

$$\begin{cases} \rho_j - \lambda \sum_{ij} v_i(t_j)\rho_i - \lambda \int K(t_j,t')y(t')dt' = f(t_j), \\ y(t) - \lambda \sum_i u_i(t)\rho_i - \lambda \int H(t,t')y(t')dt' = F(t). \end{cases} \tag{2.15}$$

The system (2.15) is in the form

$$(I - \lambda\mathbb{K})Y = R, \tag{2.16}$$

where the operators $I, \mathbb{K} : \mathbb{R}^n \times \mathcal{C} \to \mathbb{R}^n \times \mathcal{C}$; I is the identity operator, and the operator $\mathbb{K}(\rho, y) = (\xi, z)$ is defined as

$$\begin{cases} \xi_i = \sum_{ij} v_i(t_j)\rho_i - \int K(t_j, t')y(t')dt', \\ z(t) = \sum_i u_i(t)\rho_i - \int H(t, t')y(t')dt'. \end{cases} \tag{2.17}$$

It is trivial to show that the system (2.15) is equivalent to (2.1).

The operator $\mathbb{K}$ has four parts $\mathbb{K}_{11} : \mathbb{R}^n \to \mathbb{R}^n$, $\mathbb{K}_{12} : \mathcal{C} \to \mathbb{R}^n$, $\mathbb{K}_{21} : \mathbb{R}^n \to \mathcal{C}$, $\mathbb{K}_{22} : \mathcal{C} \to \mathcal{C}$, and every part is a compact operator. We use the following theorem from [7] cited here for the convenience of the reader. This theorem is formulated for a general operator $\mathbb{K}$ and space X.

Theorem *Let X be a Banach space, let $\mathbb{K}$ be an operator from X to X with*

$$||\mathbb{K} - \mathbb{K}_n|| \to 0 \quad \text{as} \quad n \to \infty$$

for some sequence of bounded, finite rank operators $\{\mathbb{K}_n\}$, and let $\lambda \neq 0$. The equation $(\lambda - \mathbb{K})x = y$ has a solution for each $y \in X$ iff the homogeneous equation $(\lambda - \mathbb{K})x = 0$ has only the trivial solution.

It is rather trivial to construct $\{\mathbb{K}_n\}$ which converges to $\mathbb{K}$ given by (2.17) in the norm

$$||\varphi|| = \max_i |\rho_i| + \max_t |y(t)|.$$

Any numerical scheme (e.g. Simpson's rule) for integration gives the desired finite dimensional approximation for $\mathbb{K}_{12}$ $\mathbb{K}_{22}$. The operator $\mathbb{K}_{11}$ is finite dimensional already and does not need to be approximated. Finally, in $\mathbb{K}_{21}$ each of the n functions

can be approximated using, for example, piecewise linear interpolation. Applying the cited theorem completes the proof.

QED

Remark This proof also suggests the numerical scheme for solving (2.1).

2.3 The 2-Dimensional Case

In the context of the physical model described in Chapter 1, we are interested in the case where φ, g and f are defined on $D = [a_1, b_1] \times [a_2, b_2]$, and K is defined on D^2. It turns out that in the two-dimensional case we can still use an approach similar to the one described in the previous section. In this section, we will redefine many variables, however their meaning will be analogous to the ones in Section 1.

We assume that the set of (t_1, t_2) such that $g(t_1, t_2) = 0$ can be parameterized by some function $h(t)$: for every t_1, there is one and only one $t_2 = h(t_1) \in [a_2, b_2]$ s.t. $g(t_1, t_2) = 0$. Such a restrictive condition is assumed for simplicity of our arguments. A more general case is considered in the next section. Note that if g is continuous, the definition of h implies that h is continuous.

The definition of N_ε, the ε-neighborhood around zeros of $g(t_1, t_2)$, changes as follows. It is a strip in the rectangular region D:

$$N_\varepsilon = \{(t_1, t_2) | t_1 \in [a_1, b_1] \text{ and } t_2 \in [h(t_1) - \varepsilon\nu(t_1), h(t_1) + \varepsilon\nu(t_1)]\},$$

where the continuous function $\nu(t_1)$ defined on $[a, b_1]$ is positive for all $t_1 \in [a_1, b_1]$.

Theorem Assume that, for some $\varepsilon > 0$,

(c1) g is continuous in D and twice differentiable in t_2 inside N_ε.

(c2) range$(h) \subset (a_2, b_2)$,

(c3) $\inf_{N_\varepsilon} \frac{\partial}{\partial t_2} g(t_1, t_2)| = M_1 > 0$,

(c4) $\sup_{N_\varepsilon} |\frac{\partial^2}{\partial t_2^2} g(t_1, t_2)| = M_3 < \infty$,

(c5) K is continuous in D^2,

(c6) $\frac{\partial}{\partial t_2'} K(t, t')$ exists in $D \times N_\varepsilon$, $\sup_{D \times N_\varepsilon} |\frac{\partial}{\partial t_2'} K(t, t')| = M_2 < \infty$,

(c7) $\frac{\partial^2}{\partial t_2 \partial t_2'} K(t, t')$ exists in $D \times N_\varepsilon$, is continuous at least at one point inside $D \times N_\varepsilon$, and $\sup_{D \times N_\varepsilon} |\frac{\partial^2}{\partial t_2 \partial t_2'} K(t, t')| = M_4 < \infty$,

(c8) the derivative $\frac{\partial}{\partial t_2} K(t, t')$ exists in $N_\varepsilon \times D$, $\sup_{N_\varepsilon \times D} |\frac{\partial}{\partial t_2} K(t, t')| = M_5 < \infty$.

(c9) $f \in \mathcal{C}(D)$ and $\frac{\partial f}{\partial t_2}$ exists in N_ε.

Then the equation

$$g(t)\varphi(t) - \lambda \int_{a_1}^{b_1} \int_{a_2}^{b_2} K(t, t')\varphi(t') dt_1' dt_2' = f(t) \tag{2.18}$$

can be viewed as $(I - \lambda \mathbb{K})Y = R$, with I being the identity operator, and $\mathbb{K}$ being a compact operator, and it has a solution for each $y \in X$ iff the homogeneous version of this equation has only the trivial solution.

Proof The idea of this proof is very similar to the proof of Theorem 1, and we will skip the explanation of the most obvious steps. In general, trivial generalizations of Lemmas 4 and 5 for the higher dimensional case can still be proved and used in the proof of this theorem.

We will look for the solution of equation (2.18) in the form

$$\varphi(t) = \rho(t)/g(t) + y(t). \tag{2.19}$$

We substitute (2.19) into (2.18):

$$\rho(t_1) + g(t)y(t) - \lambda \int_{a_1}^{b_1} P.V. \int_{a_2}^{b_2} \frac{K(t, t_1', t_2')}{g(t_1', t_2')} dt_2' \rho(t_1') dt_1' \\ -\lambda \int_{a_1}^{b_1} \int_{a_2}^{b_2} K(t, t') y(t') dt_1' dt_2' = f(t), \tag{2.20}$$

So we define the integral over the singularity as an integral over t_1 of the inner integral over t_2, and the last one is understood in the principle value sense.

Define

$$v(t, t_1') = P.V. \int_{a_2}^{b_2} \frac{K(t, t_1', t_2')}{g(t_1', t_2')} dt_2'. \tag{2.21}$$

Lemma 4 gives continuity of $v(t, t_1')$ in $N_\varepsilon \times [a_1, b_1]$.

By evaluating (2.20) at $t_2 = h(t_1)$, we obtain

$$\rho(t_1) - \lambda \int_{a_1}^{b_1} v(t_1, h(t_1), t_1') \rho(t_1') dt_1' \\ -\lambda \int_{a_1}^{b_1} \int_{a_2}^{b_2} K(t_1, h(t_1), t') y(t') dt_1' dt_2' = f(t_1, h(t_1)). \tag{2.22}$$

We subtract (2.22) from (2.20)

$$g(t)y(t) - \lambda \int_{a_1}^{b_1} [v(t_1, t_2, t_1') - v(t_1, h(t_1), t_1')] \rho(t_1') dt_1' \\ -\lambda \int_{a_1}^{b_1} \int_{a_2}^{b_2} [K(t_1, t_2, t') - K(t_1, h(t_1), t')] y(t') dt_1' dt_2' \\ = f(t_1, t_2) - f(t_1, h(t_1)). \tag{2.23}$$

Now we can divide (2.23) by $g(t)$

$$y(t) - \lambda \int_{a_1}^{b_1} \frac{v(t_1, t_2, t_2') - v(t_1, h(t_1), t_2')}{g(t)} \rho(t_1') dt_1'$$

$$
\begin{aligned}
&-\lambda \int_{a_1}^{b_1} \int_{a_2}^{b_2} \frac{K(t_1, t_2, t') - K(t_1, h(t_1), t')}{g(t)} y(t') dt'_1 dt'_2 \\
&= \frac{f(t_1, t_2) - f(t_1, h(t_1))}{g(t)}.
\end{aligned} \tag{2.24}
$$

For the sake of brevity, we define

$$
\begin{aligned}
u(t, t'_1) &= \frac{v(t_1, t_2, t'_1) - v(t_1, h(t_1), t'_1)}{g(t)}, \\
H(t, t') &= \frac{K(t_1, t_2, t') - K(t_1, h(t_1), t')}{g(t)}, \\
F(t) &= \frac{f(t_1, t_2) - f(t_1, h(t_1))}{g(t)}.
\end{aligned} \tag{2.25}
$$

Lemma 5 guarantees that $\frac{\partial v}{\partial t_2}$ is defined in $N_\varepsilon \times [a_1, b_1]$, therefore u is continuous.

Now we can rewrite (2.24) as

$$
y(t) - \lambda \int_{a_1}^{b_1} u(t, t'_1) \rho(t'_1) dt'_1 - \lambda \int_{a_1}^{b_1} \int_{a_2}^{b_2} H(t, t') y(t') dt'_1 dt'_2 = F(t), \tag{2.26}
$$

and we can view (2.22) and (2.26) as one equation $(I - \lambda \mathbb{K})Y = R$ with I being the identity map, and $\mathbb{K}$ being a map from $\mathcal{C}([a_1, b_1]) \times \mathcal{C}(D)$ into itself. Since each part of the operator $\mathbb{K}$ is compact and allows finite dimensional approximations, the same holds for $\mathbb{K}$ itself. We can apply the theorem from the previous section and conclude that the system of equations (2.22) and (2.26) has a unique solution for every right-hand side iff the homogeneous version of (2.18) has only the trivial solution.

QED

2.4 Generalizations

Some rather trivial generalizations of the 2nd theorem can be obtained with simple changes of variables. We only outline these generalization without formulating theorems.

(1) A proper change of variables allows us to consider cases where D is not bounded and not necessarily rectangular because any regularly shaped connected set is diffeomorphic to a rectangular region.

(2) If the curve formed by the roots of $g(t_1, t_2) = 0$ does not intersect itself, a proper change of variables allows us to parameterize this curve. One can transform the original IE (2.18) to this new set of variables and apply Theorem 2. Some care must be taken to insure that the definition of the principle value integral does not depend on the change of variables.

(3) The set of solutions $g(t_1, t_2) = 0$ can consist of more than one curve. In this case, we have to introduce in Theorem 2 functions analogous to p_i with similar properties. The case where a curve bifurcates is not a trivial generalization and requires further study.

(4) The dimension of the problem can be higher. It is possible to consider the n-dimensional case where the solution of $g(t)$ forms an (n-1)-dimensional manifold or manifolds. This very straightforward generalization can be obtained if we consider the variable t_1 in Theorem 2 as multidimensional.

(5) We can consider the variable t_2 as multidimensional as well and parameterize the manifold of the solutions of $g(t) = 0$ by $h : \mathbb{R}^m \to \mathbb{R}^{n-m}$. In this case, the manifold $\{t|g(t) = 0\}$ can have any number of dimensions between 0 and n-1.

To summarize, this treatment of integral equations of the 3rd kind can be generalized to the multidimensional case. The set of zeros of $g : \mathbb{R}^n \to \mathbb{R}$ can be a union

of smooth manifolds, not necessarily of the same dimension. The only restriction is that these manifolds do not change dimension and do not bifurcate.

2.5 Auxiliary Results

In this section, we prove lemmas used in Sections 1 and 2. Here we use real analysis theorems sometimes without explicitly stating them. The reader is expected to know the theorems that allow exchanges in the order of taking limits (*uniform convergence and continuity* theorem), integration (*uniform convergence and integration* theorem), and differentiation (*uniform convergence and differentiation* theorem). These classical results can be found, for example, in [8].

Lemma 1. The integral

$$P.V. \int_{-1}^{1} \frac{f(x,\lambda)}{x} dx$$

converges uniformly in λ if

$$\sup_{x \in [-\varepsilon,\varepsilon] \text{ all } \lambda} |\frac{\partial}{\partial x} f(x,\lambda)| = M < \infty.$$

Proof

$$P.V. \int_{-1}^{1} \frac{f(x,\lambda)}{x} dx = \lim_{\varepsilon \to 0} \left(\int_{-1}^{-\varepsilon} \frac{f(x,\lambda)}{x} dx + \int_{\varepsilon}^{1} \frac{f(x,\lambda)}{x} dx \right).$$

We make changes of variables in the first integral

$$\frac{dx}{x} = d \ln -x = ds, \qquad x = -e^s,$$

and in the second integral

$$\frac{dx}{x} = d \ln x = ds, \qquad x = e^s.$$

Then

$$P.V.\int_{-1}^{1}\frac{f(x,\lambda)}{x}dx=\lim_{R\to 0}\int_{-R}^{0}(-f(-e^s,\lambda)dx+f(e^s,\lambda)dx),$$

and we can estimate

$$|-f(-e^s,\lambda)dx+f(e^s,\lambda)dx|\le|\frac{\partial}{\partial x}f(\theta,\lambda)|2e^s\le 2Me^s.$$

Therefore the integral converges absolutely uniformly in λ.

QED

Lemma 2. If the following conditions hold

(1) $g(y_0)=0$,

(2) $g\in\mathcal{C}_1[y_0-\varepsilon,y_0+\varepsilon]$,

(3) $|g''(y_0)|$ exists (and finite),

then

$$\left(\frac{d}{dy}\frac{y-y_0}{g(y)}\right)\Big|_{y=y_0}=-\frac{g''(y_0)}{2[g'(y_0)]^2}.$$

Proof We use Taylor's formula in Peano's form:

$$g(y)=g(y_0)+g'(y_0)(y-y_0)+\frac{1}{2}g''(y_0)(y-y_0)^2+o((y-y_0)^2).$$

$$\frac{d}{dy}\frac{y-y_0}{g(y)}=\frac{d}{dy}\frac{y-y_0}{g'(y_0)(y-y_0)+\frac{1}{2}g''(y_0)(y-y_0)^2+o((y-y_0)^2)}=$$

$$=\frac{d}{dy}\frac{1}{g'(y_0)+\frac{1}{2}g''(y_0)(y-y_0)+o(y-y_0)}.$$

Therefore

$$\left(\frac{d}{dy}\frac{y-y_0}{g(y)}\right)\Big|_{y=y_0}=-\frac{\frac{1}{2}g''(y_0)}{(g'(y_0))^2}.$$

Here we used the fact that

$$\left(\frac{d}{dy}o(y-y_0)\right)\Big|_{y=y_0}=0.$$

QED

Lemma 3. If A is such that $y_0 \notin A$, then, for $y \in A$,

$$\frac{d}{dy}\frac{y-y_0}{g(y)} \le \frac{3\sup_{y\in A}|g''(y)|/2}{2[\inf_{y\in A}|g'(y)|]^2}.$$

Proof

$$\begin{aligned}\frac{d}{dy}\frac{y-y_0}{g(y)} &= \frac{g(y)-g'(y)(y-y_0)}{g^2(y)}\\ &= \frac{g(y)-g'(y_0)(y-y_0)+(g'(y_0)-g'(y))(y-y_0)}{g^2(y)}\\ &= \frac{g''(y_1^*)(y-y_0)^2/2-g''(y_2^*)(y-y_0)^2}{[g'(y_3^*)(y-y_0)]^2} = \frac{g''(y_1^*)/2-g''(y_2^*)}{[g'(y_3^*)]^2},\end{aligned}$$

where $y_1^*, y_2^*, y_3^* \in [y, y_0]$. Now the desired estimate is trivial.

QED

Lemma 4. If conditions (r1-7) hold, then

$$v_i(t) = P.V.\int \frac{K(t,t')p_i(t')}{g(t')}dt' \tag{2.27}$$

is continuous on $[a,b]$, and the principle value integral converges uniformly.

Proof It is enough to show that the following integral converges uniformly in t as $\varepsilon' \to 0$ (while $\varepsilon' \in (0,\varepsilon)$):

$$\left(\int_{t_k-\varepsilon}^{t_k-\varepsilon'} + \int_{t_k+\varepsilon'}^{t_k+\varepsilon}\right)\frac{K(t,t')p_j(t')}{g(t')}dt'$$

$$= \left(\int_{t_k-\varepsilon}^{t_k-\varepsilon'} + \int_{t_k+\varepsilon'}^{t_k+\varepsilon} \right) \frac{1}{t'-t_k} \left[K(t,t')p_j(t') \frac{t'-t_k}{g(t')} \right] dt'.$$

We estimate

$$\left| \frac{\partial}{\partial t'} \left[K(t,t')p_j(t') \frac{t'-t_k}{g(t')} \right] \right| \leq M_2 \sup_{t' \in N_\varepsilon} |p_j(t')| \frac{1}{M_1} + \sup_{t,t' \in N_\varepsilon} |K(t,t')| \sup_{t' \in N_\varepsilon} |p_j'(t')| \frac{1}{M_1}$$
$$+ \sup_{t \in [a,b], t' \in N_\varepsilon} |K(t,t')| \sup_{t' \in N_\varepsilon} |p_j(t')| \left| \sup_{t' \in N_\varepsilon} \frac{d}{dt'} \frac{t'-t_k}{g(t')} \right|.$$

We use Lemmas 2 and 3 to estimate

$$\left| \sup_{t' \in N_\varepsilon} \frac{d}{dt'} \frac{t'-t_k}{g(t')} \right| \leq \frac{3M_3}{2M_1^2}.$$

Now, using Lemma 1, we can conclude that the integral in (2.7) converges uniformly in t. This also allows us to exchange limits

$$\lim_{t \to t^*} \lim_{\varepsilon' \to 0} \left(\int_{t_k-\varepsilon}^{t_k-\varepsilon'} + \int_{t_k+\varepsilon'}^{t_k+\varepsilon} \right) \frac{K(t,t')p_j(t')}{g(t')} dt'$$
$$= \lim_{\varepsilon' \to 0} \lim_{t \to t^*} \left(\int_{t_k-\varepsilon}^{t_k-\varepsilon'} + \int_{t_k+\varepsilon'}^{t_k+\varepsilon} \right) \frac{K(t,t')p_j(t')}{g(t')} dt'.$$

Obviously $\int_{[a,b]\setminus N_\varepsilon} \frac{K(t,t')p_j(t')}{g(t')} dt'$ is continuous in t. Therefore v_i is continuous in t.

QED

Lemma 5. If the conditions (r1-8) hold, then $v_i \in \mathcal{C}_1(N_\varepsilon)$.

Proof Since

$$\frac{K(t,t')p_j(t')}{g(t')} \quad \text{and} \quad \frac{\partial}{\partial t} \left(\frac{K(t,t')p_j(t')}{g(t')} \right)$$

are continuous in $N_\varepsilon \times [a,b]\setminus N_{\varepsilon'}$,then

$$\frac{\partial}{\partial t} \int_{[a,b]\setminus N_{\varepsilon'}} \frac{K(t,t')p_j(t')}{g(t')} dt' = \int_{[a,b]\setminus N_{\varepsilon'}} \frac{\partial}{\partial t} \frac{K(t,t')p_j(t')}{g(t')} dt'.$$

The functions and variables in Lemma 4 can have different meanings than in this Lemma. If we apply lemma 4 to $\frac{\partial K}{\partial t}$ in place of K, then we can conclude that the integral in the right-hand side of the last equation converges uniformly in t as $\varepsilon' \to 0$. Therefore we can exchange the operators $\frac{\partial}{\partial t}$ and $\lim_{\varepsilon' \to 0}$:

$$\frac{\partial}{\partial t} \lim_{\varepsilon' \to 0} \int_{[a,b] \setminus N_{\varepsilon'}} \frac{K(t,t')p_j(t')}{g(t')} dt' =$$
$$\lim_{\varepsilon' \to 0} \frac{\partial}{\partial t} \int_{[a,b] \setminus N_{\varepsilon'}} \frac{K(t,t')p_j(t')}{g(t')} dt' = \lim_{\varepsilon' \to 0} \int_{[a,b] \setminus N_{\varepsilon'}} \frac{\partial}{\partial t} \frac{K(t,t')p_j(t')}{g(t')} dt'.$$

The last expression is known to converge uniformly in t as $\varepsilon' \to 0$ and to be continuous once (r8) holds because of Lemma 4.

QED

References

[1] R. Warnock, M. Venturini, J.A. Ellison, *Nonsingular integral equation for stability of a bunched beam,* Proceedings of EPAC 2002, Paris, France.

[2] R. Warnock, G. Stupakov, M. Venturini, J.A. Ellison, *Linear Vlasov Analysis for stability of a bunched beam,* Proceedings of EPAC, Lucerne, Switzerland, 2004.

[3] K.M. Case, *Plasma oscillations,* Ann. Physics, 7 (1959), pp. 349-364.

[4] N.G. van Kampen, *On the theory of stationary waves in plasma,* Physica 21 (1955) pp. 949-963.

[5] G.R. Bart and R.L. Warnock, *Linear integral equations of the third kind,* SIAM J. Math. Anal. Vol. 4, No. 4 (1973) pp. 609-622.

[6] G.R. Bart, *Three theorems on third-kind linear integral equations,* J. Math. Anal. and Appl. Vol. 79, No. 1 (1981) pp. 48-57.

[7] K. E. Atkinson, *A Survey of Numerical Methods for the Solution of Fredholm Integral Equations of the Second Kind,* SIAM, Philadelphia, 1976.

[8] W. Rudin, *Principles of Mathematical Analysis,* 3rd Ed. McGraw-Hill, New York, 1976.

Chapter 3

Averaging Approach for Evolving Distributions

3.1 Introduction

The method of averaging is often applied to systems of the form

$$\dot{x} = \varepsilon f(t,x) + \varepsilon^2 R(t,x,\varepsilon), \quad x(t_0) = x_0, \tag{3.1}$$

where $f(t,x)$ is periodic in t. In order to obtain an approximate solution of (3.1), it is natural to average $f(t,x)$ over t keeping x fixed and solve

$$\dot{y} = \varepsilon \bar{f}(y), \quad x(t_0) = x_0. \tag{3.2}$$

One then usually proves that $y(t)$ is an order $O(\varepsilon)$ estimate of $x(t)$ on the timescale $O(1/\varepsilon)$ although sometimes different time intervals are considered, and different estimates can be obtained. The averaging approach can also be applied to evolution

equations of the form

$$x_{n+1} = x_n + \varepsilon f(x_n, n\theta), \tag{3.3}$$

where x_0 is given, and similar results can be obtained. This method was already used as early as the 18th century by Lagrange and Laplace for studying secular perturbations of the solar system. Originally formulated for x evolving in $\mathbb{R}^m$, this approach was applied for x evolving in more general spaces such as Banach spaces [1]. A large number of results relaxing smoothness and periodicity conditions on f has been obtained during 20th century. Special techniques have been developed for finite-dimensional Hamiltonian systems, and for the Schrödinger equation [2] Averaging methods were studied for weakly nonlinear parabolic [3, 4] and hyperbolic [5, 6] partial differential equations. A review of recent results on averaging methods for PDE is given in [7]. Higher order approximations for ODE are also available [8, 9]. Historical and bibliographical information about earlier work on averaging methods can be found in [10]. The averaging approach has been previously applied to study the beam dynamics in the so-called *weak-strong* case [11, 12], where the changing of the density of the *strong* beam is neglected and the problem reduces to tracking the trajectories of the particles in the *weak* beam from turn to turn.

In this chapter, we study the density evolution under collective beam-beam effects (the *strong-strong* case) in particle colliders. Unlike the weak-strong case, which can be studied considering particle position independently, here we study the density evolving as a whole; the evolving elements become infinite-dimensional. Unlike most of the results in the literature on averaging, we study a discrete-time evolving system. The closest continuous-time system would be the nonlinear integro-differential transport equation. We rigorously prove the classical $O(\varepsilon)$ estimate on the time scale $O(1/\varepsilon)$ for the evolving functions $\Psi_n : \mathbb{R}^{m_1} \to \mathbb{R}^{m_2}$. The components of Ψ_n represent the densities of m_2 beams evolving as n, the number of turns, increases. The

theorems we prove here apply to the model with two beams ($m_2 = 2$) and densities defined in 4-dimensional phase-space ($m_1 = 4 \times 2$) as described in Chapter 1. The theorems formulated in Section 3.2 however allow arbitrary m_1 and m_2, therefore the results also apply to a more generalized model with more bunches, more interaction points, and densities evolving in 6-dimensional phase-space.

The full system of the evolution equations obtained in Chapter 1 (see equation (1.17)) is

$$\begin{cases} \Psi_{n+1} = \Psi_n \circ (I - \zeta R^{-n} \tilde{K}[\Psi_n^*] \circ R^n), \\ {\Psi^*}_{n+1} = {\Psi^*}_n \circ (I - \zeta R^{-n} \tilde{K}[\Psi_n] \circ R^n). \end{cases} \tag{3.4}$$

We can rewrite this system combining ($\Psi_n(z)$, $\Psi_n^*(z^*)$) in one vector $\mathbf{\Psi_n}(\mathbf{z})$, which depends on $\mathbf{z} = (z, z^*)$:

$$\mathbf{\Psi}_{n+1}(\mathbf{z}) = \mathbf{\Psi}_n \circ (\mathbf{z} - \zeta \mathbf{K}[\mathbf{\Psi}, n\bar{\nu}](\mathbf{z})), \tag{3.5}$$

where $\bar{\nu} = (\nu_x, \nu_y, \nu_x^*, \nu_y^*)$ is a vector with components that are horizontal and vertical tunes of unstarred and starred beams, and $\mathbf{K}$ is implicitly defined here. As we established in Chapter 1 in equations (1.18) and (1.21), $R^{-n}\tilde{K}[\Psi_n^*] \circ R^n$ has a representation

$$R^{-n}\tilde{K}[\Psi] \circ R^n(v) = \int \nabla_v H(v - v', n\bar{\nu})\, \Psi(v')dv'. \tag{3.6}$$

(One can show that ∇_v and $\int$ can be exchanged.) In the next section, we will consider evolution equations slightly more general than (3.5). We will allow $\mathbf{\Psi}$, $\mathbf{z}$, and $\bar{\nu}$ to have arbitrarily many dimensions. To simplify the notation, we will use H instead of $\nabla_v H$, and the regular font for $\mathbf{\Psi}$, $\mathbf{z}$, and $\bar{\nu}$. We use indexes to refer to the components of these vectors.

3.2 Averaging Approximation Theorems

To simplify notation throughout this chapter, we use $L(f)$ as a shorthand for a Lipschitz constant for symbol f:

$$L(f) = \sup_{x,x'} \frac{||f(x) - f(x')||}{||x - x'||}, \tag{3.7}$$

and the norms are understood from the context according to symbol f. For multi-indexes, vectors α of dimension m_3 with integer components, we define a shorthand for the norm and differential operator:

$$|\alpha| = |\alpha_1| + ...|\alpha_{m_3}|, \qquad D_s^\alpha = \frac{\partial^{|\alpha|}}{\partial s_1^{\alpha_1} ... \partial s_{m_3}^{\alpha_{m_3}}}. \tag{3.8}$$

Let H be a matrix-valued function $H : \mathbb{R}^{m_1+m_1+m_3} \to \mathbb{R}^{m_1 \times m_2}$. Define a map $K[\Psi, s] : \mathbb{R}^{m_1} \to \mathbb{R}^{m_1}$ that depends on a smooth function $\Psi : R^{m_1} \to \mathbb{R}^{m_2}$ and a vector $s \in \mathbb{R}^{m_3}$:

$$K[\Psi, s](x) = \int H(x, y, s)\Psi(x + y)dy. \tag{3.9}$$

When the set that we take the integral over is omitted, it is implied to be $\mathbb{R}^{m_1}$ throughout this chapter. Let Ψ_n be a sequence of smooth functions $\Psi_n : R^{m_1} \to \mathbb{R}^{m_2}$ satisfying the evolution equation

$$\Psi_{n+1} = \Psi_n \circ (I + \varepsilon K[\Psi_n, n\theta]) \tag{3.10}$$

with some known Ψ_0. We transform (3.10) to the equation

$$\Phi_{n+1} = \Phi_n \circ (I + \varepsilon \bar{K}[\Phi_n] + \varepsilon^2 R[\Phi_n, n, \varepsilon]), \tag{3.11}$$

and then drop the order ε^2 term. The equation obtained in this way (the so-called *averaged equation*) has a solution that is close to the solution of the original equation. The transformation from (3.10) to (3.11) is done by the so-called *near-identity transformation*

$$\Psi_n = \Phi_n \circ [I + \varepsilon P[\Phi_n, n]], \tag{3.12}$$

where $P[\Phi_n, n] : R^{m_1} \to R^{m_1}$.

Next we will derive a recursive equation for P using the following trivial property.

Lemma For two functions F_1 and F_2,

$$[I + \varepsilon F_1] \circ [I + \varepsilon F_2](x) = [I + \varepsilon F_1 + \varepsilon F_2 + \varepsilon^2 R](x), \tag{3.13}$$

where the expression for R is given by

$$R(x) = [F_1(x + \varepsilon F_2(x)) - F_1(x)]/\varepsilon. \tag{3.14}$$

This statement is particularly useful when the functions F_1 and F_2 are Lipschitz, and F_2 is bounded. Using the expressions for Ψ_n and Ψ_{n+1} given by (3.12), we rewrite (3.10) as

$$\Phi_{n+1} \circ (I + \varepsilon P[\Phi_{n+1}, n+1]) = \Phi_n \circ (I + \varepsilon P[\Phi_n, n]) \circ (I + \varepsilon K[\Psi_n, n\theta]). \tag{3.15}$$

We express Φ_{n+1} using (3.11) in the left-hand side, in order to get

$$\begin{aligned} &\Phi_n \circ (I + \varepsilon \bar{K}[\Phi_n] + \varepsilon^2 R[\Phi_n, n, \varepsilon]) \circ \\ &\quad (I + \varepsilon P[\Phi_n \circ \{I + \varepsilon \bar{K}[\Phi_n] + \varepsilon^2 R[\Phi_n, n\varepsilon]\}, n+1]) \\ &\quad = \Phi_n \circ (I + \varepsilon P[\Phi_n, n]) \circ (I + \varepsilon K[\Psi_n, n\theta]). \end{aligned} \tag{3.16}$$

This expression will be satisfied if the maps following Φ_n are identical. We use the identity (3.13) in (3.16) and keep only the ε-order terms:

$$\varepsilon\bar{K}[\Phi_n] + \varepsilon P[\Phi_n \circ (I + \varepsilon\bar{K}[\Phi_n] + \varepsilon^2 R[\Phi_n, n, \varepsilon], n+1] \\ = \varepsilon P[\Phi_n, n] + \varepsilon K[\Psi_n, n\theta] + O(\varepsilon^2) \tag{3.17}$$

Assume that $P[\Phi, n]$ is Lipschitz in Φ:

$$||P[\Phi + \Delta\Phi, n](x) - P[\Phi, n](x)||_\infty \leq L_\Phi(P)||\Delta\Phi||. \tag{3.18}$$

Here $||\Delta\Phi||$ can be either the L_2 or the uniform norm. From (3.17), we obtain a recursive relation for P:

$$P[\Phi, n+1] = P[\Phi, n] + K[\Phi, n\theta] - \bar{K}[\Phi]. \tag{3.19}$$

Without loss of generality, we can set $P[\Phi, 0] \equiv 0$. Recursive relation (3.19) implies that

$$P[\Phi, N] = \sum_{n=0}^{N-1} K[\Phi, n\theta] - \bar{K}[\Phi]. \tag{3.20}$$

It is natural to require that the term $P[\Phi, N]$ does not grow. If we assume that

$$\lim_{N\to\infty} \frac{1}{N} P[\Phi, N] = 0, \tag{3.21}$$

then it follows from (3.20) and (3.21) that

$$\bar{K}[\Phi] = \lim_{N\to\infty} \frac{1}{N} \sum_{n=0}^{N-1} K[\Phi, n\theta]. \tag{3.22}$$

In the case where θ is a vector with rational components, then for some integer m, $K[\Phi, n\theta] = K[\Phi, (n+m)\theta]$, and the choice of $\bar{K}$ is obvious:

$$\bar{K}[\Phi] = \frac{1}{m}\sum_{n=0}^{m} K[\Phi, n\theta]. \tag{3.23}$$

In the case where θ is a vector with irrational components, the existence of the $\bar{K}$ is given by the following theorem.

Theorem 1. Assume that the matrix-valued function $H(x, y, s)$ and its components $h_{ij}(x, y, s)$ satisfy the following conditions:

(c1) $H(x, y, s)$ is periodic in each component of s with period 1,

(c2) θ has irrational components whose ratios are also irrational,

(c3) $H(x, y, s)$ is continuous in $\{(x, y, s) : |y| > \varepsilon\}$ for all $\varepsilon > 0$.

(c4) the improper integral $\int \frac{1}{N}\sum_{n=0}^{N-1} H(x, y, n\theta)\Phi(x+y)dy$ converges uniformly in N and x,

(c5) $D_s^\alpha h_{ij}(x, y, s)$ exists, is continuous and periodic in each component of s, for all α such that $|\alpha| \leq m_3$,

(c6) $D_s^\alpha h_{ij}(x, y, s)$ exists and is piecewise continuous in s, for all α such that $|\alpha| = m_3 + 1$,

(c7) for some function $C(y)$ independent from s, and x,

$$|D_s^\alpha h_{ij}(x, y, s)| < C(y), \text{ for all } \alpha \text{ such that } |\alpha| \leq m_3 + 1$$

Then for continuous Φ, the operator $\bar{K}[\Phi]$ satisfying (3.22) exists and given by

$$\bar{K}[\Phi] = \int \bar{H}(x, y)\Phi(x+y)dy, \text{ where } \bar{H}(x, y) = \int_0^1 H(x, y, s)ds. \tag{3.24}$$

Note that, in this theorem, we allow the kernel to have singularities in y, which is essential in the physical applications. Theorem 1 gives sufficient conditions for the existence of $\bar{K}[\Phi]$ satisfying (3.22). However to fulfill the assumptions we made about P being bounded, we need the following stronger theorem.

Theorem 1b. Assume that $h_{ij}(x, y, s)$ satisfy the the conditions (c1-c3) of the previous theorem, and for some integer $r > 0$,

(c5') $D_s^\alpha h_{ij}(x, y, s)$ exists, is continuous, and periodic in in each component of s, for all α such that $|\alpha| \leq m_3 + r$,

(c6') $D_s^\alpha h_{ij}(x, y, s)$ exists and is piecewise continuous in s, for all α such that $|\alpha| = m_3 + r + 1$,

(c7') for some constant C,

$$|D_s^\alpha h_{ij}(x, y, s)| < C, \text{ for all } \alpha \text{ such that } |\alpha| \leq m_3 + r + 1 \ ,$$

(c8) There is some $M_5 > 0$ such that for all k, $|\exp\{2\pi i k \cdot \theta\} - 1||k|^r \geq M_5$.

Then P is a bounded operator in Φ uniformly in N:

$$||P[\Phi, n]||_\infty \leq C_1 ||\Phi||_1, \text{ for some } C_1. \tag{3.25}$$

Remark If $|r| > m_3 + 1$, then it is easy to prove that the set of θ satisfying the condition (c8) is not empty, therefore the theorem is not vacuous.

Our goal is to show that Φ_n can be approximated with $\bar{\Phi}_n$, which is a sequence of distributions $\bar{\Phi}_n$ evolving according to

$$\bar{\Phi}_{n+1} = \bar{\Phi}_n \circ (I + \varepsilon \bar{K}[\bar{\Phi}_n]), \ \bar{\Phi}_0 = \Phi_0. \tag{3.26}$$

Theorem 2. Assume that the components of the matrix $\bar{H}$ and vector $\bar{\Phi}_0$ satisfy

$$\max_{i,j} \sup_{x,x'} \int |\bar{h}_{ij}(x,y) - \bar{h}_{ij}(x',y)|dy/||x-x'|| = M_2 < \infty, \tag{3.27}$$

$$\sup_{y,j} |\varphi_{0,j}(y)| = M_3 < \infty. \tag{3.28}$$

Then

$$L(\bar{\Phi}_n) \leq L(\bar{\Phi}_0) \exp\{\varepsilon M_2 M_3 m_1 m_2 n\}. \tag{3.29}$$

Theorem 3. Assume that the conditions of Theorem 1b and 2 hold, and

$$\max_{ij} \sup_{x} \int |\bar{h}_{ij}(x,y)|dy = M_1 < \infty \text{ for all } x. \tag{3.30}$$

Assume that n is of order $O(1/\varepsilon)$, i.e. for some M_4,

$$n \leq \frac{M_4}{m_1 m_2 M_2 M_3 \varepsilon}. \tag{3.31}$$

Then $||\Phi_n - \bar{\Phi}_n||_\infty \to 0$ as $\varepsilon \to 0$.

3.3 Proofs

Proof of Theorem 1. To prove this theorem, we will analyze (3.23) by components. We will show that if the limit can be taken inside the integral, it can be calculated as in the conclusion of the theorem (3.24). Then we will show that exchanging the integration and limit is a valid operation.

From the conditions (c5-c7), it follows that the Fourier coefficients

$$h_{ij}^k(x,y) = \int_{[0,1]^{m_3}} e^{2\pi i k \cdot s} h_{ij}(x,y,s)ds$$

satisfy $|h_{ij}^k(x,y)| < C|k|^{-m_3-1}$. Using this inequality, we can estimate

$$\frac{1}{N}\sum_{n=0}^{N-1}\sum_{k:|k|=L'}^{L} |\exp\{2\pi ink\cdot\theta\}h_{ij}^k(x,y)| \le \frac{1}{N}\sum_{n=0}^{N-1}\sum_{k:\ |k|=L'}^{L} C(y)|k|^{-m_3-1}$$
$$= C(y)\sum_{k:\ |k|=L'}^{L} |k|^{-m_3-1} \to 0 \ \text{ as } \ L, L' \to \infty. \qquad (3.32)$$

This means that $\frac{1}{N}\sum_{n=0}^{N}\sum_{k:\ |k|=0}^{L}\exp\{2\pi ink\cdot\theta\}h_{ij}^k(x,y)$ converges as $L\to\infty$ uniformly in N. The other limit exists:

$$\frac{1}{N}\sum_{n=0}^{N-1}\sum_{k:\ |k|=0}^{L}\exp\{2\pi ink\cdot\theta\}h_{ij}^k(x,y) = \sum_{k:\ |k|=0}^{L}\frac{1}{N}\frac{e^{2\pi iNk\cdot\theta}-1}{e^{2\pi ik\cdot\theta}-1}h_{ij}^k(x,y)\to 0$$

as $N\to 0$. Therefore both of the following double limits exist and are equal:

$$\lim_{N\to\infty}\lim_{L\to\infty}\frac{1}{N}\sum_{n=0}^{N-1}\sum_{k:\ |k|=0}^{L}\exp\{2\pi ink\cdot\theta\}h_{ij}^k(x,y)$$
$$= \lim_{L\to\infty}\lim_{N\to\infty}\frac{1}{N}\sum_{n=0}^{N-1}\sum_{k:\ |k|=0}^{L}\exp\{2\pi ink\cdot\theta\}h_{ij}^k(x,y).$$

The right-hand side and the left-hand side of the last equality are

$$\text{L.H.S.} = \lim_{N\to\infty}\frac{1}{N}\sum_{n=0}^{N-1}\lim_{L\to\infty}\sum_{k:\ |k|=0}^{L}\exp\{2\pi ink\cdot\theta\}h_{ij}^k(x,y)$$
$$= \lim_{N\to\infty}\frac{1}{N}\sum_{n=0}^{N-1}h_{ij}(x,y,n\theta),$$
$$\text{R.H.S.} = \lim_{L\to\infty}\sum_{k:\ |k|=0}^{L}h_{ij}^k(x,y)\lim_{N\to\infty}\frac{1}{N}\sum_{n=0}^{N-1}\exp\{2\pi ink\cdot\theta\} = h_{ij}^0(x,y).$$

The last equality holds because for all $k\neq 0$

$$\lim_{N\to\infty}\frac{1}{N}\sum_{n=0}^{N-1}\exp\{ink\cdot\theta\} = \lim_{N\to\infty}\frac{1}{N}\frac{e^{2\pi iNk\cdot\theta}-1}{e^{2\pi ik\cdot\theta}-1} = 0, \qquad (3.33)$$

and if $k = 0$, the same limit equals 1. This implies that the limit

$$\lim_{N\to\infty} \frac{1}{N} \sum_{n=1}^{N} H(x, y, n\theta)\Phi(x + y) \tag{3.34}$$

exists and is continuous. Because sums and products of continuous functions are continuous functions, $\frac{1}{N}\sum_{n=1}^{N} H(x, y, n\theta)\Phi(x+y)$ is continuous in the set $\{(x, y, N) : |y| > \varepsilon\}$ for all $\varepsilon > 0$.

The last two conclusions along with Condition (c4) of the theorem allow us to exchange the integration and limit:

$$\begin{aligned}
&\lim_{N\to\infty} \int_{\mathbb{R}^{m_1}} \frac{1}{N} \sum_{n=1}^{N} H(x, y, n\theta)\Phi(x + y)dy \\
&\qquad = \int_{\mathbb{R}^{m_1}} \lim_{N\to\infty} \frac{1}{N} \sum_{n=0}^{N-1} H(x, y, n\theta)\Phi(x + y)dy \\
&\qquad = \int_{\mathbb{R}^{m_1}} \bar{H}(x, y, n\theta)\Phi(x + y)dy.
\end{aligned} \tag{3.35}$$

QED

Proof of Theorem 1b. The conditions (c5'-c7') are stronger than (c5-c7), therefore we can repeat the steps of the proof of Theorem 1, and obtain

$$\lim_{N\to\infty} \frac{1}{N} \sum_{n=1}^{N} h_{ij}(x, y, n\theta), = h^0_{ij}(x, y). \tag{3.36}$$

Let us estimate the kernel of P:

$$S(x, y, N) = \sum_{n=0}^{N-1} \sum_{k:\ |k|>0}^{L} \exp\{2\pi i n k \cdot \theta\} = \sum_{k:\ |k|>0}^{L} \frac{e^{2\pi i N k\cdot\theta} - 1}{e^{2\pi i k\cdot\theta} - 1} h^k_{ij}(x, y). \tag{3.37}$$

We can also obtain $|h_{ij}^k(x,y)| < C|k|^{-m_3-r-1}$.

$$\sum_{k:\ |k|>L'}^{L} \left| \frac{e^{2\pi i N k\cdot\theta}-1}{e^{2\pi i k\cdot\theta}-1} h_{ij}^k(x,y) \right| \le \sum_{k:\ |k|>L'}^{L} \left| e^{2\pi i N k\cdot\theta}-1 \right| \frac{|k|^r}{M_5} C|k|^{-m_3-r-1}$$
$$\le \sum_{k:\ |k|>L'}^{L} \frac{2C}{M_5}|k|^{-m_3-1} \to 0$$

as $L' \to \infty$. Therefore (3.37) converges absolutely and uniformly in x and y. Applying Hölder's inequality yields the conclusion of the theorem.

QED

Corollary The assumptions of Theorem 1b also imply conclusions of Theorem 1 because (3.21) implies (3.22).

Proof of Theorem 2. It immediately follows from (3.26) that

$$\sup_y |\bar{\varphi}_{n,j}(y)| \le M_3. \tag{3.38}$$

We can estimate

$$L(\bar{\Phi}_{n+1}) \le L(\bar{\Phi}_n) L(I + \varepsilon \bar{K}[\bar{\Phi}_n])) \le L(\bar{\Phi}_n)(1 + \varepsilon L(\bar{K}[\bar{\Phi}_n])). \tag{3.39}$$

$$\begin{aligned} L(\bar{K}[\bar{\Phi}_n]) &= \sup_{x,x'} || \int H(x,y)\bar{\Phi}(y)dy - \int H(x',y)\bar{\Phi}(y)dy||/||x-x'|| \\ &= \sup_{x,x'} || \int (H(x,y) - H(x',y))\bar{\Phi}_n(y)dy||/||x-x'|| \end{aligned} \tag{3.40}$$

$$= \sup_{x,x'} \left[\sum_{i=1}^{m_1} \left[\int \sum (\bar{h}_{ij}(x,y) - \bar{h}_{ij}(x',y))\bar{\varphi}_{n,j}(y)dy \right]^2 \right]^{1/2} /||x-x'||$$

$$\leq \sup_{x,x'} \left[\sum_{i=1}^{m_1} \left[\sum \frac{\int |\bar{h}_{ij}(x,y) - \bar{h}_{ij}(x',y)| dy}{||x-x'||} \sup_y |\bar{\varphi}_{n,j}(y)| \right]^2 \right]^{1/2}$$
$$\leq M_2 M_3 m_1 m_2. \tag{3.41}$$

Using (3.41), we continue (3.39) to obtain the recursive estimate

$$L(\bar{\Phi}_n) \leq L(\bar{\Phi}_{n-1})(1+\varepsilon M_2 M_3 m_1 m_2) \leq L(\bar{\Phi}_0)(1+\varepsilon M_2 M_3 m_1 m_2)^n, \tag{3.42}$$

and the conclusion of the theorem follows:

$$L(\bar{\Phi}_n) \leq L(\bar{\Phi}_0) \exp\{\varepsilon M_2 M_3 m_1 m_2 n\}. \tag{3.43}$$

QED

We use the following Lemma in the proof of Theorem 3.

Lemma 1. Assume that a sequence $\{x_n\}_{n=0}^{\infty}$ satisfies

$$x_n \leq x_{n-1}(1+\varepsilon a) + \varepsilon^2 b,$$

where $\varepsilon a > 0$. Then

$$x_n \leq (x_0 + \varepsilon b/a) e^{a\varepsilon n} - \varepsilon b/a.$$

Proof We can estimate

$$x_n \leq x_0(1+\varepsilon a)^n + \varepsilon^2 b \sum_{k=0}^{n-1} (1+\varepsilon a)^k \leq x_0(1+\varepsilon a)^n + \varepsilon^2 b \frac{(1+\varepsilon a)^n - 1}{\varepsilon a}$$
$$\leq (1+\varepsilon a)^n (x_0 + \varepsilon b/a) - \varepsilon b/a.$$

QED

Corollary In the case where $x_0 = 0$, $a > 0$, and $b > 0$, the following simpler estimate can be useful:

$$x_n \leq \varepsilon b e^{a\varepsilon n}/a.$$

Proof of Theorem 3. Using the triangle inequality, we can estimate

$$\begin{aligned}
||\Phi_{n+1} - \bar{\Phi}_{n+1}||_\infty &= \sup_x ||\Phi_n \circ (I + \varepsilon \bar{K}[\Phi_n] + \varepsilon^2 R[\Phi_n, n, \varepsilon])(x) \\
&\qquad -\bar{\Phi}_n \circ (I + \varepsilon \bar{K}[\bar{\Phi}_n])(x)|| \\
&= \sup_x ||\Phi_n \circ (I + \varepsilon \bar{K}[\Phi_n] + \varepsilon^2 R[\Phi_n, n, \varepsilon])(x) \\
&\quad -\bar{\Phi}_n \circ (I + \varepsilon \bar{K}[\Phi_n] + \varepsilon^2 R[\Phi_n, n, \varepsilon])(x) \\
&\quad +\bar{\Phi}_n \circ (I + \varepsilon \bar{K}[\Phi_n] + \varepsilon^2 R[\Phi_n, n, \varepsilon])(x) \\
&\quad -\bar{\Phi}_n \circ (I + \varepsilon \bar{K}[\bar{\Phi}_n] + \varepsilon^2 R[\Phi_n, n, \varepsilon])(x) \\
&\quad +\bar{\Phi}_n \circ (I + \varepsilon \bar{K}[\bar{\Phi}_n] + \varepsilon^2 R[\Phi_n, n, \varepsilon])(x) - \bar{\Phi}_n \circ (I + \varepsilon \bar{K}[\bar{\Phi}_n])|| \\
&\leq ||\Phi_n - \bar{\Phi}_n||_\infty + L(\bar{\Phi}_n) \sup_x |||[I - \varepsilon \bar{K}[\Phi_n] + \varepsilon^2 R[\Phi_n, n, \varepsilon]](x) \\
&\quad -[I - \varepsilon \bar{K}[\bar{\Phi}_n] + \varepsilon^2 R[\Phi_n, n, \varepsilon]](x)|| \\
&\quad +L(\bar{\Phi}_n) \sup_x |||[I + \varepsilon \bar{K}[\bar{\Phi}_n] + \varepsilon^2 R[\Phi_n, n, \varepsilon]](x) - [I + \varepsilon \bar{K}[\bar{\Phi}_n]](x)|| \\
&\leq ||\Phi_n - \bar{\Phi}_n||_\infty + \varepsilon L(\bar{\Phi}_n)||\bar{K}[\Phi_n - \bar{\Phi}_n]||_\infty + \varepsilon^2 L(\bar{\Phi}_n)||R[\Phi_n, n, \varepsilon](x)||_\infty. \quad (3.44)
\end{aligned}$$

We can estimate

$$\begin{aligned}
||\bar{K}[\Phi]||_\infty &= \sup_x \frac{||\bar{K}[\Phi](x)||_2}{||x||} \\
&\leq \sup_x \left[\sum_i \left[\sum_j \int \bar{h}_{ij}(x,y)\varphi_j(y)dy \right]^2 \right]^{1/2} \\
&\leq \sup_x \left[\sum_i \left[\sum_j \int |\bar{h}_{ij}(x,y)dy| \sup_y \varphi_j(y) \right]^2 \right]^{1/2}
\end{aligned}$$

$$\leq \sup_x \left[\sum_i \left[m_2 \max_j \sum_j \int |\bar{h}_{ij}(x,y)| dy \max_j \sup_y |\varphi_j(y)| \right]^2 \right]^{1/2}$$

$$\leq m_1 m_2 \max_{ij} \sup_{xy} \int |\bar{h}_{ij}(x,y)| dy \max_j \sup_y |\varphi_j(y)|. \tag{3.45}$$

Therefore, using (3.30), we obtain

$$||\bar{K}[\Phi_n - \bar{\Phi}_n]||_\infty \leq M_1 ||\Phi_n - \bar{\Phi}_n||_\infty \tag{3.46}$$

in (3.44), and obtain

$$||\Phi_{n+1} - \bar{\Phi}_{n+1}||_\infty \leq (1 + \varepsilon L(\bar{\Phi}_n))||\Phi_n - \bar{\Phi}_n||_\infty + \varepsilon^2 L(\bar{\Phi}_n)||R[\Phi_n, n, \varepsilon](x)||_\infty. \tag{3.47}$$

Because of (3.31), $L(\bar{\Phi}_k) \leq e^{M_4}$ for all $k \leq n$. Therefore, (3.47) can be rewritten as

$$||\Phi_{n+1} - \bar{\Phi}_{n+1}||_\infty \leq (1 + \varepsilon e^{M_4})||\Phi_n - \bar{\Phi}_n||_\infty + \varepsilon^2 e^{M_4} ||R[\Phi_n, n, \varepsilon](x)||_\infty. \tag{3.48}$$

Using the corollary of the lemma, we obtain

$$||\Phi_{n+1} - \bar{\Phi}_{n+1}||_\infty \leq \varepsilon \max_{k \leq n} ||R[\Phi_k, k, \varepsilon](x)|| \exp\{e^{M_4} n\varepsilon - M_4\}. \tag{3.49}$$

Next we estimate $||R[\Phi_k, k, \varepsilon](x)||$. Writing the ε^2-order term in (3.16) gives the following expression for R:

$$R[\Phi_n, n, \varepsilon] \circ (I + \varepsilon P[\Phi_{n+1}, n+1])(x) +$$
$$\{\bar{K}[\Phi_n](x + \varepsilon P[\Phi_{n+1}, n+1](x)) - \bar{K}[\Phi_n](x)\}/\varepsilon$$
$$= \{P[\Phi_n, n](x + \varepsilon K[\Phi_n, n\theta]) - P[\Phi_n, n](x)\}/\varepsilon. \tag{3.50}$$

For ε small enough, $(x + \varepsilon P[\Phi_{n+1}, n+1](x))$ can be inverted. Since $\bar{K}[\Phi_n]$ and $P[\Phi_n, n]$ are Lipschitz, and bounded, R remains bounded. Along with estimate (3.49), this completes the proof of the theorem.

References

[1] R. Buitelaar *The method of averaging in Banach Spaces: theory and application.* Rijksuniversiteit Utrecht, Nederlands, 1993.

[2] A.B. Lemlih, J.A. Ellison *Method of Averaging for the Quantum Anharmonic Oscilator* PRL, Vol. 55, Num. 19, pp. 1950-1953, 1985

[3] J.J. Heijnekamp, M.S. Krol, F. Verhulst, *Averaging in nonlinear advective transport problems,* Math. Meth. of Appl. Sciences, 18, pp. 437-448, 1995.

[4] F. Verhulst, *Methods and Applications of Singular Perturbations: Boundary Layers and Multiple Timescale Dynamics,* Springer-Uerlag June, 2005.

[5] A.C.J. Stroucken and F. Verhulst, *The Galerkin-averaging method for nonlinear, undamped continuous systems,* Math. Meth. in the Appl. Sci. 9, pp. 580-549, 1987

[6] H. Pals, *The Galerkin-averaging method for the klein-gordon equation in two space dimensions,* Nonlinear Analysis, Theory, Methods and Applications, Vol. 27, No. 7, pp. 841-856, 1996.

[7] Ferdinand Verhulst, *On averaging methods for partial differential equations,* Workshop "Symmetry and Perturbation Theory, World Scientific, 1999.

[8] A.W. Saénz, *Higher order averaging for nonperiodic systems,* J. Math. Phys. 32 (10), Oct 1991.

[9] J.A. Ellison, Albert W. Saénz, H. Scott Dumas, *Improved Nth order order averaging theory for periodic systems,* J. of Diff. Eq. vol. 84, No. 2, April 1990.

[10] J. A. Sanders and F. Verhulst, *Averaging Methods in Nonlinear Dynamical Systems*, Springer-Verlag, New York, Berlin, Heidelberg, Tokyo, 1986.

[11] H. S. Dumas, J.A. Ellison, M. Vogt *First-order averaging principles for maps with applications to beam dynamics in particle accelerators*, SIADS, Vol. 3 Num 4, pp. 409-432. 2004.

[12] H.S. Dumas, J.E. Ellison, *Averaging for quasiperiodic systems,* Proceedings of the International Conference on Differential Equations, Hasselt, Belgium, July 22–26, 2003.

Chapter 4

The Simulation of the Strong-Strong Beam-Beam Interaction in Circular Particle Colliders by Tracking Densities in 4D Phase-Space

4.1 Introduction

The most straightforward approach, macro-particle tracking (MPT), has been successfully implemented in a number of parallel codes [1, 2, 3]. Such codes can simulate rather complicated physical models: particles with 3 DF, synchrotron radiation, finite dimensional crossing angles, and many IPs. However fully complete modeling of a real machine is still beyond current computational power. These models suffer from statistical noise, and do not directly compute the beam's densities. The neces-

sary number of particles is determined from numerical experiment rather than from analytic estimates. There is, of course, a trade-off between the number of particles and the number of the time steps (turns), and the reasonable number of time steps limits the number of macro-particles to 10^6.

Different 1 DF models have been considered [5], [6] and shown to capture important basic characteristics of beam-beam interaction. Much less computationally expensive methods that assume that the beam density can be represented as Gaussian or Hermitian polynomial [4] are able to capture some of the properties of real beams and are free from statistical noise, though they cannot capture the details of the phases-pace densities of the beams.

More sophisticated mathematical techniques can significantly improve the speed and precision of the calculations. One such technique, calculating the beam densities in slowly varying coordinates, is described in this chapter. Other techniques may utilize the autonomous continuous-time averaged Vlasov equation introduced in Chapter 3. The main idea of such improvements is to calculate numerically perturbations around some analytically obtained solutions that capture the most essential properties of the model. Here we are interested primarily in studying such essential properties rather than implementing a code that able to predict the beam evolution in some particular real accelerator.

We simulate the density evolution in the beam-beam interactions for many turns at the circular particle accelerators using the Perron-Frobenious (PF) method. In this method, the beams are represented by their densities approximated on a fixed grid, and we solve a Vlasov-type equation by tracking the density values along the particle's trajectories in a 4D phase-space. We study the evolution of the densities of two counter-rotating colliding beams with one bunch in each beam. The PF method is implemented in a parallel C++ code using MPI libraries. For solving Poisson's equation, we calculate the solution on the boundary of a rectangular uniform grid

and find the values in the interior points using the conjugate-gradient (CG) method similarly to [3].

In 1DF case, a similar approach has been successfully applied, and compared with the macro-particle tracking method in [7]. The codes for simulating collective beam-beam dynamics are hard to compare against experiments, because the beam-beam interaction is almost always designed to be weak, and the interpretation of the measurements can be obscured by other effects.

This chapter is organized as follows. First, we describe the algorithm that implements the model described in Chapter 1. The separate sections describe the data structures that represent the beams, the distribution of the data between the nodes of the parallel computer, and the communication between nodes. Finally we discuss the results of the simulations, and the code's properties such as efficiency, the preservation of probability and other quantities.

4.2 Algorithm

We have implemented evolution equations (1.15) in earlier simulation codes, however in the latest code we use the evolution equations in slowly varying coordinates (1.17). They are more suitable for the numerical simulation because of the following reasons.

First, it dramatically reduces the data exchange between the different nodes on the parallel computer performing the simulation. In order to compute the value of the $\Psi_{n+1}(z)$ using (1.15), one would need to know the values of Ψ_n that are far away from z, and the corresponding data may be located on a different node. The fact that ζ is small combined with the structure of the equation (1.17) guarantees that the values of Ψ_{n+1} can be computed using the information located on the same node for most of the gridpoints of Ψ_n. The only data that needs to be exchanged

between nodes are Ψ_n values at the points on the boundary of the region locally stored on the node. This reduces the amount of communication by the so-called "volume-to-surface" factor.

Second, computing evolution of Ψ_n does not involve computing the evolution on the rotation part. Even though the "rotation part" of the evolution is trivial in a way, it introduces the largest error. If the kick is small, the error in (1.17) is proportional to $O(\zeta^2)$ with $\zeta \approx 0.0036$, while the error in (1.13) is $O(h^2)$, where $h \approx 0.05$ is the grid step size.

We can choose the linear change of variables such that the rotation matrix is orthonormal in (1.17) or close to orthonormal. We model Ψ_n defined on $\mathbb{R}^4$, such that Ψ_0 is Gaussian, and all Ψ_n also decay very fast, so we can limit the domain to some finite rectangle. Since the density rotates in the domain, it makes sense to choose the mesh symmetric with respect to the origin. In most of our numerical experiments, we chose a rectangular mesh with a span from -5.5σ to 5.5σ in each dimension, where σ is approximately the RMS of Ψ_0. The beam density is represented as an array

$$\texttt{Psi[i][j][k][l]} = \Psi_n(z_i^1, z_j^2, z_k^3, z_l^4),$$

where z_i^s – are the gridpoints of the uniform rectangular 4 dimensional grid. To calculate the values of `Psi` on every turn, we iterate over the gridpoints and track back the coordinate of the gridpoint according to (1.17). Then we approximate the value of Ψ_n on the previous turn between the gridpoints from values of `Psi` calculated for the previous turn stored in a different array. For this approximation, we use quadratic interpolation in the 4D phasespace, which involves 81 neighboring gridpoints.

At the same time as the 4D beam density is being calculated, the spatial density

is calculated according to

$$\rho_{n+1}(x,y) = \int \Psi_{n+1} \circ R^{-n-1} \begin{pmatrix} x & x' & y & y' \end{pmatrix}^T dx'dy'. \tag{4.1}$$

The spatial density ρ is represented by a 2D array

$$\texttt{rho[i][j]} = \rho(x_i, y_j),$$

where (x_i, y_j) are the gridpoints of the uniform 2-dimensional rectangular mesh. The values of `rho` are calculated by projecting the 4D gridpoints on the (x,y)-plane and distributing the charge between the cells that corresponds to the four closest gridpoints on 2D mesh.

The potential is calculated by approximating the Laplace operator using the 5-point stencil method in $\Delta\varphi = -4\pi\rho$, and solving this linear equation using the CG method. We will not go into the details of this algorithm here, and give only a very short description for the convenience of the reader.

```
x=b;
r=Ax-b;
p:=r;
while (|r|>eps){
    k=(r,Ap)/(p,Ap);
    p=r-kp;
    a=(p,r)/(p,Ap)
    x=x-ap;
    r=Ax-b;
}
```

The boundary values can either be set to be zero or calculated using the Green function. The kick is calculated on the grid as $-\nabla\varphi$ using a 2 point finite difference method and interpolated between points using linear interpolation.

4.3 Distributing Data Between the Processes

A user specifies in the PBS file how many processors and processes must be allocated for the computation. Normally there is only one process running on each processor though for debugging purposes one may want to run many processes on one processor. Many parallel computers have several processors on each node. Here we describe the calculation in terms of processes, since it is the basic execution unit.

At the beginning of the program execution, a special MPI routing splits the available processes in two groups such that communication between the processes within the groups is the fastest. The processes in each group calculate the density of one beam on every turn, therefore each beam has its own set of processes. Each processor contains values of `Psi` approximating Ψ_n on the subdomains of the *full grid*. We call these subdomains *the process grids*. A special MPI routing helps assign each process a subdomain, therefore organizing them in a 4-dimensional grid, which we call *the grid of processes*, such that the communication between the neighbors in the grid is the fastest.

We refer to the points on the edge of the process grid as *padding*, and to the rest of the points as *owned*. The padding points that are also on the edge of the full grid are set to zero, and referred to as *zero padding*. The rapid decrease of the density justifies setting the value of `Psi` to zero at these points. We allocate memory for padding gridpoints in order to have the same procedure of calculating all gridpoints without any conditional statement in the inner *for*-loop. This requires more memory, but eliminating conditional statements and makes computation faster. The padding gridpoints that are not on the edge of the full grid are called *shared*. The coordinates of these gridpoints are the same as the coordinates of some of the owned gridpoints of the corresponding neighbor process, and the value of `Psi` at these points is communicated between the processes on every turn.

Sometimes the number of the process gridpoints is still very large, and the corresponding data does not fit the cache. In order to perform the 4-dimensional quadratic interpolation quickly, the process grid can be split into smaller subgrids. This way of reorganizing data increases the portion of data kept and retrieved from the cache, which speeds up the computation. Therefore there are three level of grids: (1) the grid of processes, (2) the process grids, and (3) the subgrids.

On every turn, each node calculates the values of `Psi` only at the gridpoints that it owns using the values of `Psi` on the previous turn at the owned gridpoints as well as at the padding gridpoints. Then the values of `Psi` at the shared gridpoints are received from the neighbor processes, where they are calculated.

To calculate the "kick", the Poisson equation is solved in parallel. The 2D arrays that approximate ρ and φ are distributed between the processes similarly to the way 4D arrays are distributed. While solving the Poisson equation, the same processes that constitute the 4D grid of processes are organized in a 2D grid. Similarly, the edge gridpoints are classified as padding and owned points. The values of `rho` at the edge of the full grid are either set to zero at the very beginning and never recalculated (*zero padding* option), or calculated using the Green function on every turn (*free boundary* option). The values at the shared gridpoints have to be received from the corresponding neighbor on every CG iteration. Besides collecting some scalar values, this is the only communication needed in the CG algorithm. The amount of data involved in solving the Poisson equation is smaller, which makes the task much easier.

In our numerical experiments, we usually choose the mesh step for the Poisson solver to be about the same size as the mesh step for Ψ, and twice as many gridpoints, such that the Poisson solver grid always spans the projection of the rotating 4D cube where Ψ is interpolated on two spacial dimensions.

4.4 Input Parameters

At the beginning of the program execution, the densities of the beams are set to have a normal distribution with arbitrary mean and covariance matrix specified as input parameters. The tunes in definition (1.14) of R are specified independently for each beam. If desired, a general 4×4 matrix R for the linear lattice can be specified. The dimensions of each level of 4D and 2D grids are specified, and the splitting of the full grid into subgrids must agree with the number of the available processors. The various parameters related to the Poisson solver, such as precision and the maximum number of iterations, are specified as input parameters as well.

This gives a rather large number of parameters. The runs take hours if not days, and some hours may pass even before the program starts executing. Thus it would be nice to have a special language for the input file, and some tool for validating its syntax, which would guarantee that the input file does not have any typos. It would be convenient for the input language to be able to perform some calculations. For example, we use tunes related to the golden mean, and it is convenient to state explicitly how these irrational numbers were calculated. Currently we have used 15 different versions of this program, adding new features to each next version, and there would be a serious issue of compatibilities of the input file format.

Surprisingly there is a very simple solution to all these problems. All desired features, such as validation and the ability to use expressions in the input file, are indeed available in C itself, and the compiler can take care of reading and interpreting the file. So the program does not have any input in the usual sense, instead all parameters are set before the main loop by calling the procedure setParam() defined in the file param.cpp, which is compiled before every run. Successful compiling guarantees that, after hours waiting in a cue, the program will not quit or produce some garbage just because there was a typo in the input file. Before compiling the

program, one must set the variable DEST_DIR in the makefile to let the compiler know where to take "param.cpp" and where to put the executable file.

Since the program is expected to be run by an experienced user and to be compiled about as many times as executed, additional compilation for "setting the parameters" does not create any significant overhead. If there will be ever a need to run this program with different parameters without recompiling, the procedure of reading an input file can, of course, be implemented.

4.5 Results of Simulations

We executed the program with the largest grid sizes set to 128 points per dimension. In 48 hours, the natural limit of execution time on `seaborg.nersc.gov`, we were able to calculate 5000 turns of 128 ppd grid using 512 nodes. The numerical experiments have shown that the smaller grids with 96 or even 60 ppd can be quite adequate. If we allocate the same amount of resources, we can calculate 14000 turns for 96 a ppd grid. For most of the runs, we used an initial offset of 0.2σ for one beam and 0 for the other. We set the mesh size for the Poisson solver to have twice as many points per dimension as the grid for Ψ. This allows us to fully cover the projection of an arbitrary rotated 4d cube on the square, assuming that the step size in the 2d and 4d meshes are the same.

It is not possible to save the full density of two beams with 128^4 gridpoints for thousands of turns. Such an amount of data can neither be stored nor directly visualized. The output of the program is two files (one for each beam). For every turn, these files contain the first and second moments of the beam distributions, the total sum of the values of `Psi` (*zero moment*), the number of CG iterations, and the precision achieved by the Poisson solver. Optionally, the 2D spatial density can be saved at the selected turns, and visualized after the program is finished. For

example, the user can select to save the spatial densities on each 10th turn from the 3000th through 5000th turns. We wrote a special tool in C++ that can create and execute a series of `gnuplot` scripts. These scripts read the files with density data and create `*.eps` files, which in turn, can be combined together using the `ImageMagick` tool called `convert` to form a single movie file with the extension `*.mpeg` or any other supported by `ImageMagick`. In addition, a separate file can be created by every process with information about code execution. These files can be used for debugging purposes in case if the process crushes.

One of the first moments of each beam can be extracted from the output, and added to form a series, which we call the σ-mode. Similarly, the difference of these moments forms the π-mode series. The discrete Fourier transform of these series gives information about the frequency spectrum of beam oscillation. It is known from experiments and has been confirmed by analytical estimates of Yokoya [4] that we must observe a certain tune shift in these spectra. In our numerical experiments, the π-mode had a tune shift close to 1.21 which is the expected tuneshift for the round beam, and the σ-mode did not have significant tune shift, which is also expected (see fig. 4.1). The 14000 turns allows a fairly good resolution in calculating the peak of the π-mode.

It is remarkable that the total number of particles (i.e. total probability) is preserved and stays within 1% of 1.0, which indicates a sufficient grid span (see Fig. 4.2). As expected, after some initial growth, the emittance stays almost a constant. The figure 4.4 indicates that the Poisson solver reaches high precision on every iteration.

Table 4.1 shows the amount of time spent per gridpoint for different grid sizes and different numbers of processors involved in the computation. This table indicates that the code is very scalable, i.e. the time spent calculating one iteration is inversely proportional to the number of processors.

ppd	proc	turn time / point
64	32	0.000111766
64	16	0.000111321
64	8	0.000110102
64	4	0.000110667
48	32	0.000116182
48	16	0.000111411

ppd	proc	turn time / point
48	8	0.000110185
48	4	0.000111356
32	32	0.000113655
32	16	0.000112052
32	8	0.000110703
32	4	9.12059E-05

Table 4.1: Calculation Time Spent per Gridpoint.

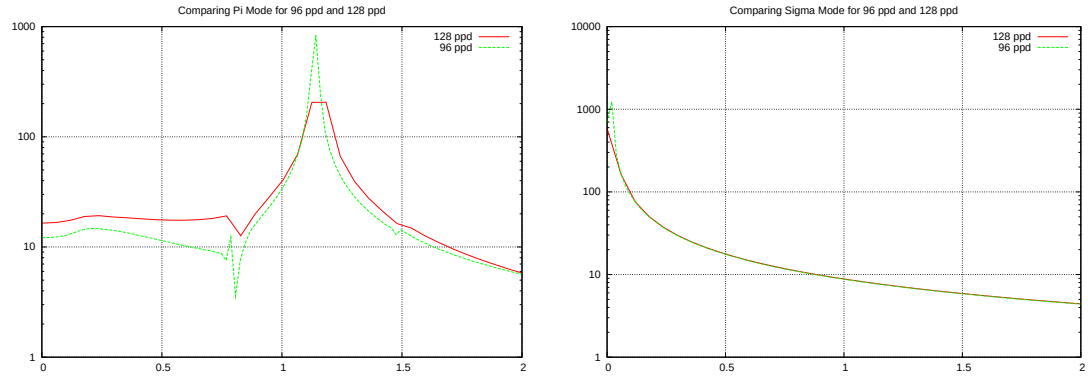

Figure 4.1: Fourier transformation of the π and σ modes for 96 ppd and 128 ppd.

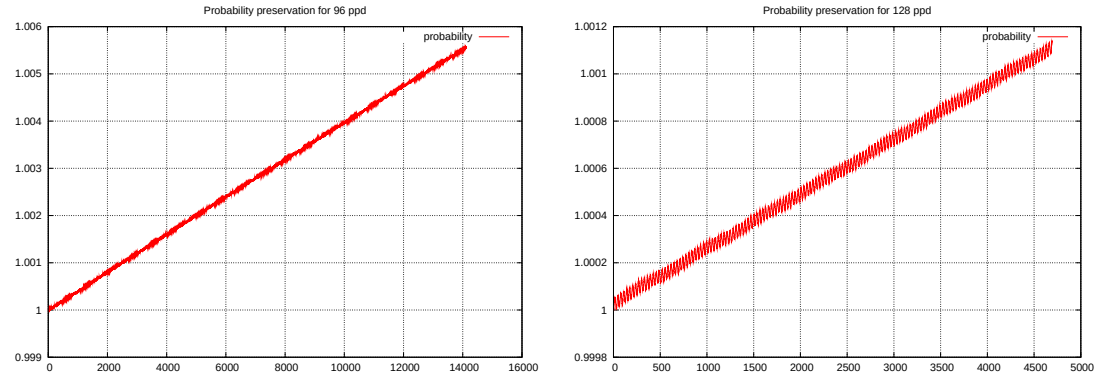

Figure 4.2: Normalization of $\int \Psi(z)dz$ on 96 and 128 ppd Meshes.

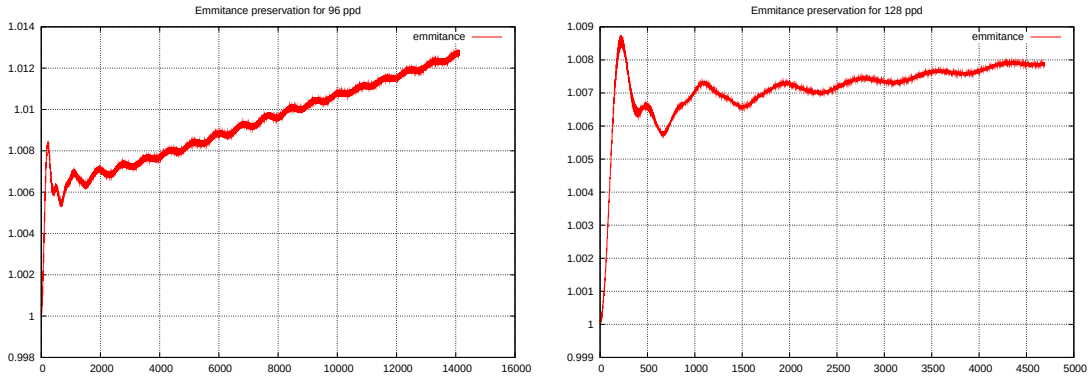

Figure 4.3: Emittance Calculation on 96 and 128 ppd Meshes

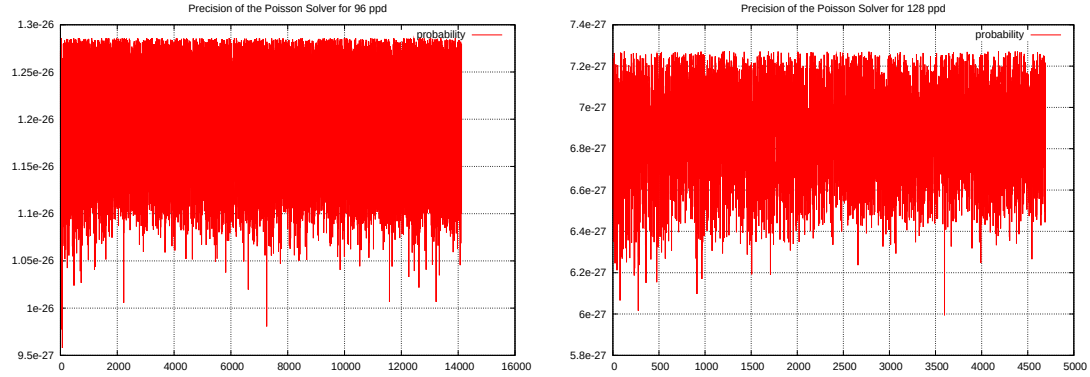

Figure 4.4: Precision in the Poisson Solver

References

[1] J. Qiang, R.D. Ryne, S. Habib, V. Decky, *An object-oriented parallel particle-in-cell code for beam dynamics simulation in linear accelerators.* Proceedings of the 1999 ACM/IEEE conference on Supercomputing.

[2] J. Qiang, M. Furman, R.D. Ryne, *Strong-strong beam-beam simulation using a Green function approach,* PRST-AB 5, 104402, 2002.

[3] Y. Cai, A.W. Chau, S.I. Tzenov, *Simulation of the beam-beam effects in e^+e^- storage rings with a method of reducing regions of mesh,* PR ST-AB, vol. 4, 011001, 2001.

[4] K. Yokoya, *Limitation of the Gaussian approximation in beam-beam simulation,* PRST-AB 3, 124401, 2000.

[5] B.S. Schmekel, G.H. Hoffstaeter, J.T. Rogers, *Investigation of the flat-beam model of the beam-beam interaction.* PRST-AB 6, 104403, 2003.

[6] M. Vogt, T. Sen, J.A. Ellison *Simulation of three one dimensional limits of the strong-strong beam interaction in hardron colliders.* Phys. Rev. ST Accel. Beams 5, 024401 (2002) and FNAL Pub-01/096-T, 2001.

[7] M. Vogt, J. Ellison, T. Sen, R. Warnock, *Two methods for simulating the strong-strong beam-beam interaction in hadron colliders,* Phys. Rev. ST Accel. Beams 5, 024401, 2002.

[8] Y. Alexahin, M.P. Zorzano, *Excitation of coherent beam-beam resonances for beams with unequal tunes in LHC,* LHC Project Note 226, June 2000.

[9] Y. Alexahin, H. Grote, W. Herr, M.P. Zorzano, *Coherent beam-beam effects in LHC,* LHC Project report 469, April 2001.

[10] K. Ohmi, *Simulation of beam-beam effects in a circular e^+e^- collider,* Physical Review E, vol. 62, No. 5, November 2000.

[11] D. Neuffer, *An analysis of the beam-beam interaction in high energy $p\bar{p}$ (pp) colliders,* Particle Accelerators, vol. 20, pp. 97-119, 1986

[12] J. A. Ellison, S. Dumas, M. Salas, T. Sen, A. Sobol, M. Vogt, *Weak-Strong Beam-Beam: Averaging and Tune Diagrams.* Conference Proceedings : Beam Halo Dynamics, Diagnostics and collimation. Workshop on Beam-Beam Interaction Beam-Beam'03. Montauk, New York, 2003.

Appendices

Appendix A

Potential Generated by the Round Gaussian Distribution

Lemma 1. The solution of

$$\Delta\varphi = -4\pi\rho(x), \qquad x \in \mathbb{R}^2 \tag{A.1}$$

$$\text{where } \rho(x) = \frac{1}{2\pi\sigma^2} \exp\left\{-\frac{|x|^2}{2\sigma^2}\right\}, \tag{A.2}$$

$$\text{is given by } \varphi(x) = U(|x|), \tag{A.3}$$

where

$$U(r) = \int_0^\infty \frac{1}{2\sigma^2 + q} \left(\exp\left\{-\frac{r^2}{2\sigma^2 + q}\right\} - 1\right) dq + C \tag{A.4}$$

with arbitrary C.

Proof First let us calculate $U'(r)$. Since $\sigma > 0$, we can exchange the differentiation and integral in (A.4):

$$U'(r) = -\int_0^\infty \frac{2r}{(2\sigma^2+q)^2} \exp\left\{-\frac{r^2}{2\sigma^2+q}\right\} dq. \tag{A.5}$$

This integral can be calculated if we change the variables:

$$s = \frac{1}{2\sigma^2+q}, \quad ds = -\frac{dq}{(2\sigma^2+q)^2}. \tag{A.6}$$

Then

$$\begin{aligned} U'(r) &= \int_{1/(2\sigma^2)}^0 2re^{-r^2 s} ds = -\frac{2}{r}\int_0^{1/(2\sigma^2)} e^{-r^2 s} d(r^2 s) \\ &= -\frac{2}{r}(-e^{-y})\Big|_{y=0}^{y=\frac{r^2}{2\sigma^2}} = \frac{2}{r}\left(\exp\left\{-\frac{r^2}{2\sigma^2}\right\} - 1\right). \end{aligned} \tag{A.7}$$

We know that the solution of (A.1) for arbitrary ρ is given by

$$\varphi(x) = \int G(x-y)\rho(y)dy, \tag{A.8}$$

where

$$G(x) = \ln(1/|x|^2). \tag{A.9}$$

Therefore we conclude that $\varphi(x)$ depends only on $|x|$, and in other words, has a representation (A.3). Now we have to verify that (A.1), (A.2), and (A.3) imply (A.4). If two functions defined on $\mathbb{R}$ have the same derivatives and coincide at one point, then they are the same. Since C is arbitrary we only have to show that (A.1), (A.2), and (A.3) imply (A.7). Define $B(R) = \{|x| < R\}$. Using consequently (A.3),

the Gauss theorem, (A.1), (A.2), we obtain

$$\begin{aligned} 2\pi R U'(R) &= \int_{\partial B(R)} \nabla\varphi \cdot n dS = \int_{B(R)} \Delta\varphi(x)dx \int_{B(R)} (-4)\pi\rho(x)dx \\ &= -4\pi \int_0^R 2\pi r\rho(r)dr = -4\pi \int_0^R 2\pi r \frac{1}{2\pi\sigma^2} e^{-\frac{r^2}{2\sigma^2}} dr \\ &= 4\pi \int_0^R e^{-\frac{r^2}{2\sigma^2}} d\left(-\frac{r^2}{2\sigma^2}\right) = 4\pi\left(e^{-\frac{R^2}{2\sigma^2}} - 1\right). \end{aligned} \tag{A.10}$$

Therefore (A.1), (A.2), and (A.3) imply

$$U'(R) = \frac{2}{R}\left(e^{-\frac{R^2}{2\sigma^2}} - 1\right). \tag{A.11}$$

Comparing the last equality with (A.7) concludes the proof.

Appendix B

Calculation of Ω

Lemma 2. The integral functional $\bar{H}$ defined in (1.19) applied to the equilibrium distribution Ψ_e defined in (1.30) is given by

$$\bar{H}[\Psi_e](J) = \int_0^\infty \frac{1}{2+q}\left(\exp\left(-\frac{J_1+J_2}{2+q}\right) I_0\left(\frac{J_1}{2+q}\right) I_0\left(\frac{J_2}{2+q}\right) - 1\right) dq.$$

Proof

$$\begin{aligned}\bar{H}[\Psi_e](J) &= \int_{\mathbb{R}_+^2}\int_{[0,2\pi]^2} \bar{G}(J, J', \theta' - \theta)\Psi_e(J', \theta')dJ'd\theta' \\ &= \int_0^\infty\int_0^{2\pi}\int_0^{2\pi}\int_0^1\int_0^1 G(D_1(J_1, J_1', \theta_1' - \theta_1)\cos 2\pi t_1, \\ &\quad D_2(J_2, J_2', \theta_2' - \theta_2)\cos 2\pi t_2)dt_1dt_2\frac{1}{4\pi^2}e^{-J_1'-J_2'}d\theta_1'd\theta_2'dJ_1'dJ_2'.\end{aligned}$$

Since the inner integral is taken over a whole period, we can add anything we want to the arguments of cos:

$$... = \int_0^\infty\int_0^{2\pi}\int_0^{2\pi}\int_0^1\int_0^1 G(D_1(J_1, J_1', \theta_1' - \theta_1)\cos(\theta_1' - \theta_1 + 2\pi t_1),$$

Appendix B. Calculation of Ω

$$D_2(J_2, J_2', \theta_2' - \theta_2)\cos(\theta_2' - \theta_2 + 2\pi t_2))dt_1 dt_2$$
$$\frac{1}{4\pi^2} e^{-J_1' - J_2'} d\theta_1' d\theta_2' dJ_1' dJ_2'$$

Again because the θ_m' run over a whole period, $\bar{H}[\Psi_e](J)$ does not depend on θ_m. We can integrate over θ_1 and θ_1 and divide by $4\pi^2$.

$$\begin{aligned} ... = \int_0^{2\pi} d\theta_1 \int_0^{2\pi} d\theta_2 \frac{1}{4\pi^2} \int_0^{\infty} dJ_1' \int_0^{\infty} dJ_2' \int_0^{2\pi} d\theta_1' \int_0^{2\pi} d\theta_2' \int_0^1 dt_2 \int_0^1 dt_1 \\ G(D_1(J_1, J_1', \theta_1' - \theta_1)\cos(\theta_1' - \theta_1 + 2\pi t_1), \\ D_2(J_2, J_2', \theta_2' - \theta_2)\cos(\theta_2' - \theta_2 + 2\pi t_2)) \frac{1}{4\pi^2} e^{-J_1' - J_2'}. \end{aligned}$$

Next we exchange the order of integration:

$$\begin{aligned} ... = \int_0^1 dt_2 \int_0^1 dt_1 \int_0^{2\pi} d\theta_1 \int_0^{2\pi} d\theta_2 \frac{1}{4\pi^2} \int_0^{\infty} dJ_1' \int_0^{\infty} dJ_2' \int_0^{2\pi} d\theta_1' \int_0^{2\pi} d\theta_2' \\ G(D_1(J_1, J_1', \theta_1' - \theta_1)\cos(\theta_1' - \theta_1 + 2\pi t_1), \\ D_2(J_2, J_2', \theta_2' - \theta_2)\cos(\theta_2' - \theta_2 + 2\pi t_2)) \frac{1}{4\pi^2} e^{-J_1' - J_2'}. \end{aligned}$$

We change variables

$$\begin{aligned} x &= \sqrt{2J_1}\cos(\theta_1 - 2\pi t_1), \qquad p_x = \sqrt{2J_1}\sin(\theta_1 - 2\pi t_1), \\ y &= \sqrt{2J_2}\cos(\theta_2 - 2\pi t_1), \qquad p_y = \sqrt{2J_2}\sin(\theta_2 - 2\pi t_1), \\ x' &= \sqrt{2J_1'}\cos(\theta_1'), \qquad p_x' = \sqrt{2J_1'}\sin(\theta_1'), \\ y' &= \sqrt{2J_2'}\cos(\theta_2'), \qquad p_y' = \sqrt{2J_2'}\sin(\theta_2'). \end{aligned} \tag{B.1}$$

(The Jacobian of the transformation is 1.)

$$... = \int_0^1 dt_2 \int_0^1 dt_1 \underbrace{\int_0^{2\pi} d\theta_2 \int_0^{2\pi} d\theta_1 \frac{1}{4\pi^2} \int_{\mathbb{R}^4} dz' \;\; G(x' - x, y' - y) \frac{1}{4\pi^2} e^{-|z'|^2/2}}_{\heartsuit},$$

where x and y must be understood as functions of t_m, θ_m, and J_m defined in (B.1). It is clear that the expression $\heartsuit$ does not depend on t_1, t_2, and therefore we can

remove the integral over these two variables. The integral over p'_x, and p'_y can be calculated:

$$... = \int_0^{2\pi} d\theta_2 \int_0^{2\pi} d\theta_1 \frac{1}{4\pi^2} \int_{\mathbb{R}^2} G(x'-x, y'-y) \frac{1}{2\pi} e^{-\frac{x^2+y^2}{2}} dx'dy'.$$

We have shown above in Appendix A that the inner integral equals

$$U(x,y) = \int_0^\infty \frac{1}{2+q} \left(\exp\left(-\frac{x^2+y^2}{2+q} \right) - 1 \right) dq. \tag{B.2}$$

Therefore

$$\begin{aligned}
... &= \int_0^{2\pi} d\theta_2 \int_0^{2\pi} d\theta_1 \frac{1}{4\pi^2} \int_0^\infty \frac{1}{2+q} \left(\exp\left(-\frac{x^2+y^2}{2+q} \right) - 1 \right) dq \\
&= \iint\limits_{[0,2\pi]^2} d^2\theta \frac{1}{4\pi^2} \int_0^\infty \frac{1}{2+q} \left(\exp\left(-\frac{(\sqrt{2J_1}\cos\theta_1)^2 + (\sqrt{2J_2}\cos\theta_2)^2}{2+q} \right) - 1 \right) dq \\
&= \iint\limits_{[0,2\pi]^2} d^2\theta \frac{1}{4\pi^2} \int_0^\infty \frac{1}{2+q} \left(\exp\left(-\frac{J_1+J_2}{2+q} \right) \right. \\
&\qquad \left. \exp\left(-\frac{J_1\cos 2\theta_1 + J_2 \cos 2\theta_2}{2+q} \right) - 1 \right) dq.
\end{aligned}$$

We used $2\cos^2\theta_m = \cos 2\theta_m + 1$ in the last equality. Now we use the Jacobi-Anger equality

$$e^{-s\cos 2\tau} = I_0(s) + 2\sum_{k=1}^{\infty} (-1)^k I_k(s) \cos 2k\tau, \tag{B.3}$$

where I_0 is the modified Bessel function, and obtain

$$\begin{aligned}
\bar{H}(J)[\Psi_e] = \int_0^{2\pi} d\theta_1 \int_0^{2\pi} d\theta_2 \frac{1}{4\pi^2} \int_0^\infty \frac{1}{2+q} \left(\exp\left(-\frac{J_1+J_2}{2+q} \right) \times \right. \\
\left[I_0(\frac{J_1}{2+q}) + 2\sum_{k=1}^{\infty} (-1)^k I_k(\frac{J_1}{2+q}) \cos 2k\theta_1 \right] \times
\end{aligned}$$

$$\left[I_0(\frac{J_2}{2+q}) + 2\sum_{k=1}^{\infty}(-1)^k I_k(\frac{J_2}{2+q})\cos 2k\theta_2 \right] - 1 \Bigg) dq$$
$$= \int_0^\infty \frac{1}{2+q}\left(\exp\left(-\frac{J_1+J_2}{2+q}\right) I_0\left(\frac{J_1}{2+q}\right) I_0\left(\frac{J_2}{2+q}\right) - 1\right) dq.$$

QED

Lemma 3. For $H[\Psi_e](J)$ given in the conclusion of the previous lemma, and $\Omega := \nabla H[\Psi_e](J)$, the expressions for $\Omega_1(J_1, 0)$ and $\Omega_1(0, 0)$ can be calculated in terms of elementary functions:

$$\Omega_1(J_1, 0) = (e^{-J_1/2} I_0(J_1/2) - 1)/J_1, \tag{B.4}$$
$$\Omega_1(0, 0) = -1/2. \tag{B.5}$$

Proof

$$\bar{H}[\Psi_e](J_1, 0) = \int_0^\infty \frac{1}{2+q}\left(\exp\left(-\frac{J_1}{2+q}\right) I_0\left(\frac{J_1}{2+q}\right) - 1\right) dq. \tag{B.6}$$

Let us change variables

$$s = \frac{J_x}{2+q}, \quad q = \tfrac{J_x}{s} - 2, \quad dq = \frac{-J_x}{s^2} ds.$$

$$\bar{H}[\Psi_e](J_1, 0) = \int_{J_1/2}^0 \frac{1}{J_x} s\{e^{-s} I_0(s) - 1\}(-\frac{J_1}{s^2}) ds = \int_0^{J_1/2} \{e^{-s} I_0(s) - 1\}/s ds,$$

$$\frac{\partial}{\partial J_1}\bar{H}[\Psi_e](J_1, 0) = \Omega_1(J_1, 0) = \frac{1}{2}(e^{-J_1/2} I_0(J_1/2) - 1)\frac{2}{J_1} = (e^{-J_1/2} I_0(J_1/2) - 1)/J_1.$$

Appendix B. Calculation of Ω

We can calculate $\Omega_1(0,0)$ using l'Hospital's rule

$$\Omega_1(J_1,0) = \lim_{J_1\to 0} \frac{\partial}{\partial J_1}(e^{-J_1/2}I_0(J_1/2) - 1) = \lim_{J_1\to 0} (-1/2)e^{-J_x/2}I_0(J_1/2) + e^{-J_1/2}I_1(J_1/2) = -1/2.$$

QED

Appendix C

Optimization of the Numerical Solution of the Integral Equation

The kernel given by (1.39) and (1.35) of the integral equation (1.40) is a function that depends on 4 variables, and in order to calculate the value at every point, a four-fold integral needs to be taken. It is impossible to do numerically unless we find an efficient way to calculate the kernel. In this appendix, we reduce the four-fold integral in (1.39) to a 2-fold integral.

We define a shorthand for part of the expression for K_k:

$$Z(A,B) = \int_0^1 \int_0^1 \ln(A\cos^2 2\pi t_x + B\cos^2 2\pi t_y) dt_x dt_y, \tag{C.1}$$

where $A > 0$, and $B > 0$, and we transform

$$Z(A,B) = \int_0^1 \int_0^1 \ln(A+B) + \ln(\frac{A}{A+B}\cos^2 2\pi t_x + \frac{B}{A+B}\cos^2 2\pi t_y) dt_x dt_y.$$

Next, we use the trivial identity

$$\cos^2\alpha = \frac{2\cos\alpha^2\alpha - 1}{2} + \frac{1}{2} = \frac{1}{2}\cos 2\alpha + \frac{1}{2}.$$

Appendix C. Optimization of the Numerical Solution of the Integral Equation

$$
\begin{aligned}
Z(A,B) &= \ln(A+B) + \int_0^1 \int_0^1 \ln\left(\frac{A}{A+B}\cos^2 2\pi t_x \right. \\
&\qquad \left. + \frac{B}{A+B}\frac{1}{2} + \frac{B}{A+B}\frac{1}{2}\cos 4\pi t_y\right) dt_x dt_y \\
&= \ln(A+B) + \int_0^1 \frac{1}{4\pi}\int_0^{4\pi} \ln(\frac{A}{A+B}\cos^2 2\pi t_x \\
&\qquad + \frac{B}{A+B}\frac{1}{2} + \frac{B}{A+B}\frac{1}{2}\cos t_y) dt_x dt_y.
\end{aligned}
$$

Using a known integral

$$
\int_0^\pi \ln(a \pm b\cos x)dx = \pi \ln\frac{a+\sqrt{a^2-b^2}}{2},
$$

we continue the equality:

$$
\begin{aligned}
&... = \ln(A+B) + \frac{1}{\pi}\int_0^1 \int_0^\pi \ln(...) dt_x dt_y \\
&= \ln(A+B) + \frac{1}{\pi}\int_0^1 \pi \ln\left(\left[\frac{A}{A+B}\cos^2 2\pi t_x + \frac{B}{A+B}\frac{1}{2} + \right.\right. \\
&\qquad \left.\left. \sqrt{\left(\frac{A}{A+B}\cos^2 2\pi t_x + \frac{B}{A+B}\frac{1}{2}\right)^2 - \left(\frac{1}{2}\frac{B}{A+B}\right)^2}\right] /2\right) dt_x \\
&= \ln(A+B) + 4F\left(\frac{B}{A+B}\right),
\end{aligned}
$$

where

$$
\begin{aligned}
F(\alpha) = \int_0^{1/4} \ln\Big(\Big[&(1-\alpha)\cos^2 2\pi t_x + \frac{\alpha}{2} \\
&+ \sqrt{\left((1-\alpha)\cos^2 2\pi t_x + \frac{\alpha}{2}\right)^2 - \frac{\alpha^2}{4}}\Big] /2\Big) dt_x.
\end{aligned}
$$

We can calculate the values of this function with arbitrary precision in the constant time using an interpolation, after we calculate the values of this function at sufficiently many gridpoints. This allows us to remove two inner integrals in the

expression for K_k. Therefore K_k is given by

$$K_k(J,J') = -\frac{1}{16\pi^4} e^{-(J_1+J_2+J_1'+J_2')/2} \int\int_{[0,2\pi)^2} d^2\theta e^{-\theta\cdot k} \left[\ln(D_1(J,J',\theta)+D_2(J,J',\theta)) + 4F\left(\frac{D_2(J,J',\theta)}{D_1(J,J',\theta)+D_1(J,J',\theta)}\right)\right].$$